

Eigenfunctions for a Spherical and a Deformed Saxon-Woods Potential*

AMAND FAESSLER† AND RAYMOND K. SHELINE

Florida State University, Tallahassee, Florida

(Received 25 February 1966)

The eigenfunctions for spherical and deformed Saxon-Woods potentials with a Thomas-type spin-orbit coupling are calculated for mass number $A=185$. The expansion coefficients into oscillator functions and the energies are tabulated for the spherical Saxon-Woods functions for $N=4$ and 5 proton shells and for $N=5$ and 6 neutron shells. For states with a binding energy >2 MeV the first six coefficients contain more than 99% of the Saxon-Woods function. The overlap integral for these states with the corresponding oscillator functions is always greater than 0.92. The basis for the spheroidal nuclei is confined to a single N shell. The deformed potential reproduces the experimental level sequence in the rare-earth nuclei using the optical-model parameters. The well depth, however, is fitted using the binding energy of the last particle. The differences between the quadrupole matrix elements in the Saxon-Woods and oscillator potentials are as large as 60% for states with a binding energy greater than 2 MeV. The γ -ray transitions between states of small binding energy and more than one node are enhanced by several oscillator units. The quadrupole matrix elements and the mixing coefficients for the rare-earth nuclei are tabulated and the expressions for the transition probabilities are given in the (jIK) representation.

1. INTRODUCTION

FOR the last fifteen years nuclear-structure calculations were inconceivable without the shell-model description for spherical^{1,2} and deformed nuclei.³ The great success of this approach brought very suitable refinement of the single-particle model involving the interaction between nucleons and the form and behavior of the self-consistent field. But most of these calculations have assumed an oscillator basis. It is well known that for small binding energies the oscillator function gives an inaccurate description of the real behavior of a nucleon. For processes which depend on the conduct of a bound state at great distances from the nucleus, e.g., radioactive capture or stripping and pickup, either a square well with a finite well depth,⁴ or a "cutoff" oscillator potential,⁵ as well as Saxon-Woods potentials have been utilized.^{6,7}

Often these refinements have less influence than the differences between the oscillator functions and the eigenfunctions for a Saxon-Woods potential. The gamma-ray transition probability between two states with small binding energies can be enhanced to several Weisskopf single-particle units by using Saxon-Woods functions, while for an oscillator basis a sophisticated

residual-interaction calculation has to be done to get a similar collective enhancement.

It seems, therefore, worthwhile to make a systematic comparison between the oscillator and the Saxon-Woods functions for the spherical and the deformed cases.

In this paper the Saxon-Woods functions for $N=4$ and 5 protons and $N=5$ and 6 neutrons are calculated for spherical and deformed fields.

In Sec. 2 the Saxon-Woods Hamiltonian with the Thomas-type spin-orbit coupling is given and the numerical method for the solution is briefly outlined. The Saxon-Woods functions are tabulated by expanding them in oscillator functions. It is shown that all functions with a binding energy greater than 2 MeV can be represented by six coefficients with accuracy better than 99%. This is, therefore, a convenient way to tabulate the Saxon-Woods wave functions. First, one does not need the lengthy tabulation of numerical values of the function and, second, the analytic expressions for the oscillator matrix elements can be used.

In Sec. 3 the formulation of the Hamiltonian of a multipole deformed Saxon-Woods potential is given. The effect of the incompressibility of nuclear matter is taken into account by volume conservation up to second order in the deformation parameters. The formulas are then restricted to a symmetric quadrupole deformation. The model yields the correct level sequence of the deformed states in the rare-earth region, including the neutron states with asymptotic quantum numbers $\frac{7}{2}+[633]$ and $\frac{1}{2}-[521]$, for which the original Nilsson model gives the wrong sequence. It also gives the right value for the decoupling parameter of the $\frac{1}{2}-[510]$ band. The mixing coefficients for mass number $A=185$ are tabulated.

In Sec. 4, γ -ray transition probabilities in the deformed region are discussed and formulas for the (jIK) representation are given in the Appendix. The matrix elements for Saxon-Woods functions and oscilla-

* Supported partially by the AEC under Contract No. AT-(40-1)-2434 and by the German "Ministerium für Wissenschaft und Forschung."

† On leave of absence from the University of Freiburg, Freiburg, Germany.

¹ O. Haxel, J. H. D. Jensen, and H. E. Suess, *Z. Physik* **128**, 295 (1950).

² M. G. Mayer, *Phys. Rev.* **75**, 1969 (1949).

³ S. G. Nilsson, *Kgl. Danske Videnskab. Selskab, Mat. Fys. Medd.* **29**, No. 16 (1955).

⁴ R. F. Christy and I. Duck, *Nucl. Phys.* **24**, 78 (1961).

⁵ R. H. Bassel, R. M. Drisko, and G. R. Satchler, Oak Ridge National Laboratory Report No. ORNL-3240 (unpublished).

⁶ P. J. Wyatt, J. G. Wills, and A. E. S. Green, *Phys. Rev.* **119**, 1031 (1960); R. H. Lemmer and A. E. S. Green, *ibid.* **119**, 1043 (1960).

⁷ R. M. Drisko and X. Rybicki, *Phys. Rev. Letters* **16**, 275 (1966).

tor functions are compared. It is found that values depend strongly on the width of the potential near the binding energy. For this reason differences between the two potentials of up to 60% are observed for the r^2 matrix elements. These matrix elements are tabulated for the rare-earth region. The Saxon-Woods matrix elements for states with a binding energy less than 2 MeV but involving more than one node are always greater than the corresponding oscillator values for positive powers of r . The $E2$ transition probability between the $4s_{1/2}$ and the $3d_{5/2}$ neutron states is enlarged by a factor of 2.85 owing to this effect and the single-particle proton quadrupole moment increases by a factor of two.

2. THE SAXON-WOODS FUNCTIONS FOR A SPHERICAL POTENTIAL

The plan of this section is to solve the Schrödinger equation for a spherical Saxon-Woods function with a Thomas-type spin-orbit coupling. These functions will be used in the next section as a convenient basis for the deformed potential. For the spherical case, elaborate analysis of the experimental data^{8,9} within the framework of the optical model has given the following form of the real potential:

$$V(r) = -V_0 f(r) + (\hbar/m\pi c)^2 C_0 \frac{1}{r} \frac{\partial}{\partial r} f(r) \mathbf{l} \cdot \mathbf{s}, \quad (1)$$

with

$$f(r) = \{1 + \exp[(r - r_0 A^{1/3})/a_0]\}^{-1}.$$

The length factor introduced in the spin-orbit term is the π -meson Compton wavelength (1.4 F). The Pauli-spin operator \mathbf{s} and the orbital angular momentum operator \mathbf{l} are given in units of \hbar . The nuclear radius, $R_0 = r_0 A^{1/3}$, is taken from the optical-model fits ($r_0 = 1.25$ F), while the diffuseness parameter a_0 is fitted by utilizing the experimental level sequence for the deformed potential. For the neutrons this value is $a_0 = 0.64$ F, which is also the best fit for the optical model. For protons the Coulomb interaction was not taken into account. (The code was originally made for neutrons only.) This interaction was simulated by

TABLE I. The fits of the well depth using the binding energy of the last particle are listed.

Proton orbits				Neutron orbits			
Nucleus	State	E_B (MeV)	V_0	Nucleus	State	E_B (MeV)	V_0
¹⁴¹ Pr	$2d_{5/2}$	5.43	36.34	¹⁴² Nd	$2f_{7/2}$	6.00	47.54
¹⁴⁷ Pm	$2d_{5/2}$	5.39	35.56	¹⁴⁶ Nd	$2f_{7/2}$	5.96	47.13
¹⁹⁷ Au	$2d_{3/2}$	6.32	34.43	¹⁴⁸ Sm	$2f_{7/2}$	5.90	48.06
²⁰³ Tl	$3s_{1/2}$	5.78	34.57	¹⁹⁵ Pt	$3p_{1/2}$	6.17	44.82
²⁰⁹ Tl	$3s_{1/2}$	6.68	35.31	¹⁹⁷ Hg	$3p_{1/2}$	6.90	45.44
				¹⁹⁹ Hg	$3p_{1/2}$	6.68	45.01
Average V_0 [MeV]			35.24	Average V_0 [MeV]			46.33

⁸ F. Bjorklund and S. Fernbach, Phys. Rev. **109**, 1295 (1958).

⁹ F. G. Perey, Phys. Rev. **131**, 745 (1963).

using a smaller well depth, V_0 , and a smaller diffuseness parameter, $a_0 = 0.52$ F. The well depth is adjusted by utilizing the binding energy of the last proton ($V_0 = 35.34$ MeV) or the last neutron ($V_0 = 46.33$ MeV) immediately before and after the deformed rare-earth region (see Table I). The spin-orbit constant was extrapolated from the optical-model fits to negative energies ($C_0 = 10$ MeV).

If one separates the solution of the Schrödinger equation into a radial and an angular part,

$$[\nu j l m] = r^{-1} u_{\nu j l} [\hat{j}]^{1/2} \times (-)^{\frac{1}{2} - l - m} \sum_{\Lambda \Sigma} \begin{pmatrix} l & \frac{1}{2} & j \\ \Lambda & \Sigma & -m \end{pmatrix} Y_{l\Lambda}(\theta, \phi) f_{\frac{1}{2}\Sigma}, \quad (2)$$

then one gets for the radial equation

$$u_{\nu j l}'' - [l(l+1)/r^2 + 2(mc/\hbar)^2 \times (mc^2)^{-1}(V(r) - E)] u_{\nu j l} = 0. \quad (3)$$

The Greek letter $\nu = 1, 2, 3, \dots$ denotes the radial quantum number, which counts the zeros, including the one at zero but not counting the zero at infinity. It is related to the radial quantum numbers of the harmonic oscillator by the equation

$$\nu = n + 1 = (N - l)/2 + 1. \quad (4)$$

The Greek capitals Λ and Σ are projections of the orbital angular momentum l and the spin, $S = \frac{1}{2}$. The caret symbol is an abbreviation for

$$\hat{j} \equiv 2j + 1. \quad (5)$$

The $3j$ and the $6j$ symbols in the notation of Edmonds¹⁰ will be used throughout this paper. If the Compton wavelength of the proton and its rest mass,

$$\begin{aligned} \hbar/(mc) &= 0.210309 \text{ F}, \\ mc^2 &= 938.211 \text{ MeV}, \end{aligned} \quad (6)$$

are written in fermis and in MeV, respectively, then the parameters V_0 and C_0 must be written in MeV in the potential

$$V(r) = -V_0 f(r) + C_0 (1.4)^2 \times \frac{1}{r} \frac{\partial}{\partial r} f(r) \times \begin{cases} l & \text{for } j = l + \frac{1}{2} \\ -l - 1 & \text{for } j = l - \frac{1}{2} \end{cases} \quad (7)$$

and the coordinate r must be used in units of fermis. The radial equation (3) is solved by the method described by Hartree,¹¹ but the Haming method¹² is used instead of the Numerov method, for the numerical integration.

¹⁰ A. R. Edmonds, *Angular Momentum in Quantum Mechanics* (Princeton University Press, Princeton, New Jersey, 1957).

¹¹ D. R. Hartree, *The Calculation of Atomic Structures* (John Wiley & Sons, Inc., New York, 1957).

¹² A. Ralston and H. S. Wilf, *Mathematical Methods for Digital Computers* (John Wiley & Sons, Inc., New York, 1960), p. 95.

FIG. 1. The Saxon-Woods potential in units of V_0 and its first two derivatives are compared with the oscillator potential in the same units. The distance from the center of the nucleus is given in units of R_0 ($R_0=7.12$ F). The diffuseness parameter has the value $a_0=0.64$ F. The oscillator potential is normalized to the $1i_{13/2}$ state for $\hbar\omega=41/(185)^{1/3}$ MeV.

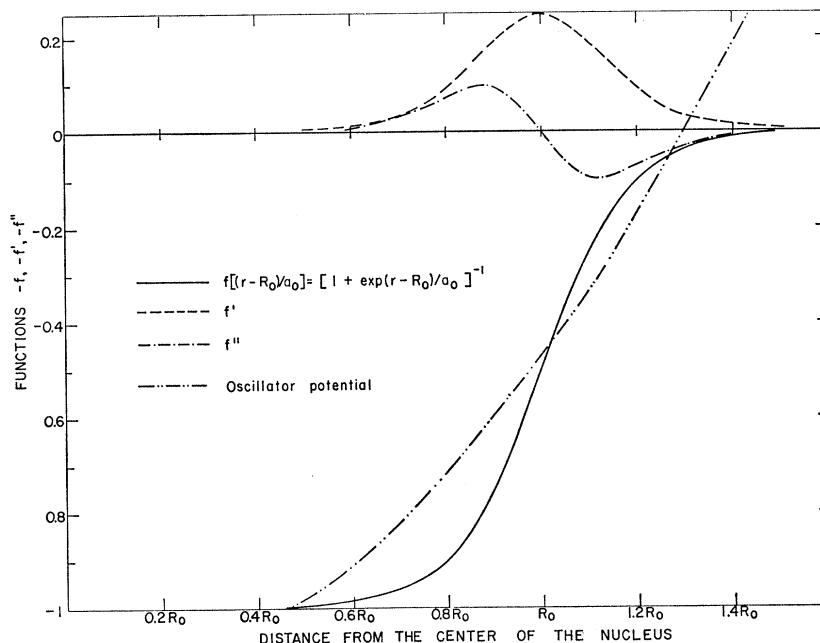


Figure 1 shows the potential in units of V_0 and its derivatives for $R_0=1.25 \times 185^{1/3}=7.12$ F and a diffuseness parameter $a_0=0.64$ F. It is compared with the oscillator potential in the same units for the oscillator energy $\hbar\omega=41/185^{1/3}$ MeV. The oscillator potential does not fit the Saxon-Woods potential for negative energies too well. In particular, it is too wide at the average binding energy of about $6 \text{ MeV} \approx V_0/8$.

In Fig. 2 the single particle energies for the $N=4$ and $N=5$ shells for the protons and the $N=5$ and $N=6$ shells for the neutrons are compared with the spherical energies of Nilsson.³

The experimental values for the hole states in ^{207}Pb and for the particle states in ^{209}Pb are normalized to the $3p_{1/2}$ (the notation $\nu l j$ is used) and to the $4s_{1/2}$ of the Saxon-Woods potential, respectively. The theoretical levels are for the mass number $A=185$, so that the $2g_{7/2}$ and the $3d_{3/2}$ are already unbound, while these states are still bound in Pb.

In Fig. 3 the eigenfunctions for the $4s_{1/2}$ and $3d_{5/2}$ neutron states and the $1g_{7/2}$ and $1h_{11/2}$ proton states are compared with the corresponding oscillator functions. The difference in the exponential tail for the Saxon-Woods functions and the Gaussian slope for the oscillator solution can be seen for neutron wave functions, which have a small binding energy. For greater binding energy the functions are surprisingly similar.

The energies of the Saxon-Woods functions and the expansion coefficients into oscillator functions are tabulated in Table II. (Such an expansion has also been studied by Sliv and Volchok¹³.) For all states with a

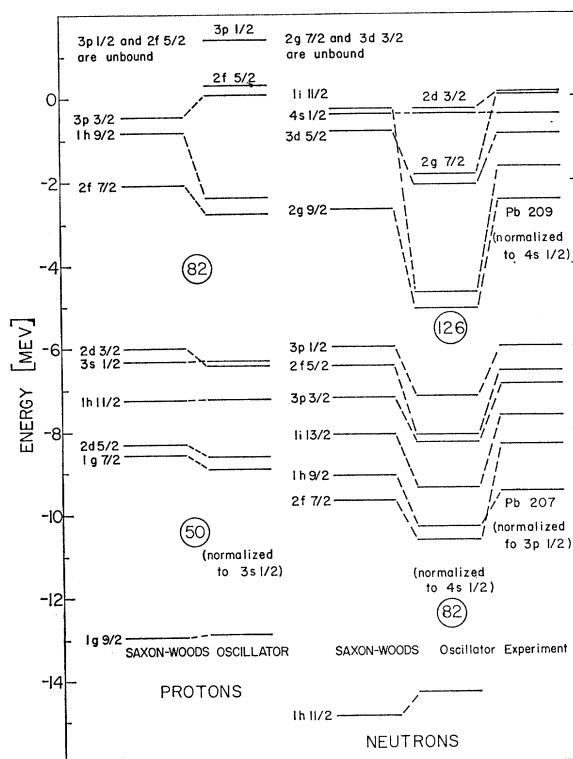


FIG. 2. The single-particle energies for the spherical Saxon-Woods potential and the oscillator potential (with the Nilsson parameters) are compared for the mass number $A=185$. For the Saxon-Woods potential the proton states $3p_{1/2}$ and $2f_{5/2}$ and the neutron states $2g_{7/2}$ and $3d_{3/2}$ are unbound, while the corresponding states for the mass number $A=208$ are bound. This is important in comparing the particle and the hole neutron states in ^{209}Pb and ^{207}Pb with this calculation.

¹³ L. A. Sliv and B. A. Volchok, Zh. Eksperim. i Teor., Fiz. 36, 539 (1959), [English transl.: Soviet Phys.—JETP 9, 374 (1959)].

TABLE II. The energies and the first six coefficients for the expansion into oscillator functions $|\nu = \frac{1}{2}(N-l)+1, l\rangle$ are tabulated for the Saxon-Woods eigenfunctions $|\nu l j\rangle$ with mass number $A=185$. In the last column the percentage of how well the first six coefficients represent the Saxon-Woods function is given. The parameters for the potential are $r_0=1.25$ F, $C_0=10$ MeV, $V_0=35.24$ MeV, $a_0=0.52$ F for the protons, and $r_0=1.25$ F, $V_0=46.33$ MeV, $C_0=10$ MeV and $a_0=0.64$ F for the neutrons.

State νl_j	E [MeV]	$\nu=1$	$\nu=2$	$\nu=3$	$\nu=4$	$\nu=5$	$\nu=6$	%
Proton orbits								
$1g_{9/2}$	-12.96	0.9836	0.1552	-0.0837	0.0232	0.0255	-0.0147	99.99
$1g_{7/2}$	-8.57	0.9969	-0.0099	-0.0496	0.0576	-0.0011	-0.0087	99.5
$2d_{5/2}$	-8.32	-0.2853	0.9336	0.1982	-0.0592	0.0519	0.0336	99.95
$2d_{3/2}$	-6.02	-0.1983	0.9688	0.1169	-0.0303	0.0814	0.0218	99.98
$3s_{1/2}$	-6.31	0.0733	-0.2710	0.9299	0.2173	-0.0244	0.0801	99.7
$1h_{11/2}$	-7.27	0.9921	0.0814	-0.0765	0.0514	0.0171	-0.0162	99.99
$1h_{9/2}$	-0.83	0.9935	0.0771	0.0182	0.0789	-0.0074	0.0105	99.97
$2f_{7/2}$	-2.09	-0.2128	0.9481	0.1958	0.0073	0.1126	0.0540	99.8
$3p_{3/2}$	-0.46	0.0753	-0.1746	0.8216	0.3299	0.1651	0.2304	90.0
Neutron orbits								
$1h_{11/2}$	-14.88	0.9945	-0.0489	-0.0730	0.0540	-0.0024	-0.0120	99.98
$1h_{9/2}$	-9.08	0.9818	-0.1810	0.0048	0.0524	-0.0225	0.0049	99.999
$2f_{7/2}$	-9.68	-0.1207	0.9877	-0.0156	-0.0580	0.0775	0.0001	99.97
$2f_{5/2}$	-6.44	-0.0190	0.9920	-0.0889	0.0060	0.0850	-0.0119	99.9
$3p_{1/2}$	-7.24	0.0711	-0.1028	0.9863	0.0298	-0.0225	0.0991	99.9
$3p_{3/2}$	-6.00	0.0675	-0.0555	0.9900	0.0087	0.0098	0.1071	99.9
$1i_{13/2}$	-8.11	0.9896	-0.1205	-0.0384	0.0653	-0.0156	-0.0048	99.98
$1i_{11/2}$	-0.28	0.9703	-0.2218	0.0783	0.0471	-0.0197	0.0207	99.98
$2g_{9/2}$	-2.70	-0.0368	0.9926	-0.0247	0.1222	0.1085	0.0051	99.9
$3d_{5/2}$	-0.81	0.0750	-0.0189	0.9403	0.1539	0.1306	0.1974	97.0
$4s_{1/2}$	-0.41	-0.0023	0.0746	-0.0083	0.7964	0.2546	0.2247	73.0

binding energy of 2 MeV and greater, the first six coefficients contain more than 99% of the Saxon-Woods function. This occurs in spite of the fact that, e.g., the $2d_{5/2}$ proton state has an overlap of -0.28 and 0.20 with the next lower and next higher shell of the same parity. With this tabulation one has not only the advantage of representing the wave function with only 6 numbers, but also one can use the analytic expressions for the oscillator matrix elements. Furthermore, it is possible with no great loss of accuracy, as has been verified in a number of cases (see Table III), to use the tabulated wave functions for the neighboring mass numbers by choosing the appropriate oscillator constant

$$\alpha = [\hbar/(m\omega)]^{1/2}, \quad (8)$$

with

$$\hbar\omega = 41A^{-1/3} [\text{MeV}].$$

The phases of the Saxon-Woods and the oscillator functions are chosen such that the tail is always positive. With this choice the oscillator functions have

TABLE III. Dependence of the $\frac{1}{2} - [510]$ neutron state on mass number.

$\frac{1}{2} - [510]$	$C_{1/2,1}$	$C_{3/2,1}$	$C_{5/2,3}$	$C_{7/2,2}$	$C_{9/2,5}$	$C_{11/2,5}$
$A=169$	0.173	0.634	0.559	-0.326	-0.380	0.070
$A=173$	0.153	0.639	0.563	-0.332	-0.368	0.073
$A=177$	0.135	0.643	0.566	-0.338	-0.357	0.075
$A=181$	0.118	0.647	0.568	-0.344	-0.347	0.077
$A=185$	0.102	0.651	0.569	-0.849	-0.337	0.079
$A=193$	0.074	0.657	0.571	-0.358	-0.320	0.082

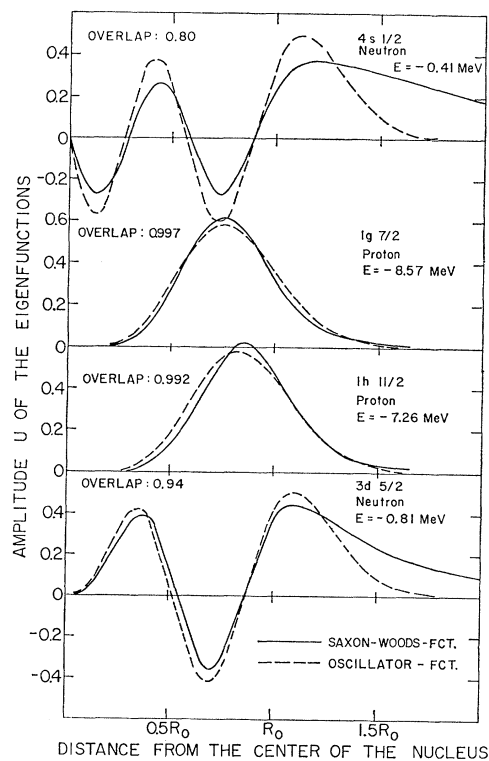


FIG. 3. The same oscillator and the Saxon-Woods functions are compared for our choice of parameters. The energy and the overlap integral $\langle \text{oscillator} | \text{Saxon-Woods} \rangle$ is given.

the same phase as in the Nilsson paper³:

$$|\nu jlm\rangle = r^{-1} v_{\nu l}(\rho) (-)^{\frac{1}{2}-l-m} j^{1/2} \sum_{\Lambda\Sigma} \begin{pmatrix} l & \frac{1}{2} & j \\ \Lambda & \Sigma & -m \end{pmatrix} Y_{l\Lambda}(\theta, \phi) \chi_{\frac{1}{2}\Sigma}; \quad (9)$$

with

$$v_{\nu l}(\rho) = (-)^{\nu-1} [2\Gamma(\nu+l+\frac{1}{2})/(\nu-1)!]^{1/2} \Gamma^{-1}(l+\frac{3}{2}) \rho^{l+1} e^{-\frac{1}{2}\rho^2} {}_1F_1(-\nu+1, l+\frac{3}{2}, \rho^2)$$

$$\rho = r/\alpha = r - \frac{mc}{\hbar} \left(\frac{\hbar\omega}{mc^2} \right)^{1/2},$$

$$\nu = 1, 2, 3, \dots,$$

and

$$\int_0^\infty v_{\nu l}^2(\rho) d\rho = 1.$$

Nilsson³ gives a very useful formula for the calculation of matrix elements of ρ^λ for $l+l'+\lambda = \text{even}$:

$$\langle \nu' l' | \rho^\lambda | \nu l \rangle = \left[\frac{\Gamma(\nu)\Gamma(\nu')}{\Gamma(\nu+l-\tau)\Gamma(\nu'+l-\tau')} \right]^{1/2} \tau! \tau'! \sum_{\sigma} \frac{\Gamma(t+\sigma+1)}{\sigma!(\nu-\sigma-1)!(\nu'-\sigma-1)(\sigma+\tau-\nu+1)(\sigma+\tau'-\nu'+1)!}, \quad (10)$$

where

$$\begin{aligned} \tau &= \frac{1}{2}(l'-l+\lambda), & \tau' &= \frac{1}{2}(l-l'+\lambda), \\ t &= \frac{1}{2}(l+l'+\lambda+1), \end{aligned} \quad (11)$$

and the summation variable is limited by

$$\left. \begin{matrix} \nu-1 \\ \nu'-1 \end{matrix} \right\} \geq \sigma \geq \left\{ \begin{matrix} \nu-\tau-1 \\ \nu-\tau'-1 \end{matrix} \right. \quad (12)$$

If no σ fulfills relation (12), then the integral is zero.

Some of the most important special cases of Eq. (10) are the following:

$$\begin{aligned} \langle \nu, l-1 | r | \nu, l \rangle &= (\nu+l-\frac{1}{2})^{1/2}, \\ \langle \nu-1, l+1 | r | \nu, l \rangle &= (\nu-1)^{1/2}, \\ \langle \nu+1, l-1 | r | \nu, l \rangle &= \nu^{1/2}, \\ \langle \nu, l+1 | r | \nu, l \rangle &= (\nu+l+\frac{1}{2})^{1/2}, \end{aligned} \quad (13)$$

and

$$\begin{aligned} \langle \nu, l | r^2 | \nu, l \rangle &= 2\nu+l-\frac{1}{2} = N+\frac{3}{2}, \\ \langle \nu+1, l-2 | r^2 | \nu, l \rangle &= 2[\nu(\nu+l-\frac{1}{2})]^{1/2}, \\ \langle \nu-1, l+2 | r^2 | \nu, l \rangle &= 2[(\nu-1)(\nu+l+\frac{1}{2})]^{1/2}, \\ \langle \nu-1, l | r^2 | \nu, l \rangle &= [(\nu-1)(\nu+l-\frac{1}{2})]^{1/2}, \\ \langle \nu, l-2 | r^2 | \nu, l \rangle &= [\nu(\nu+l+\frac{1}{2})]^{1/2}, \\ \langle \nu, l-2 | r^2 | \nu, l \rangle &= [(\nu+l-\frac{1}{2})(\nu+l-\frac{3}{2})]^{1/2}, \\ \langle \nu, l+2 | r^2 | \nu, l \rangle &= [(\nu+l+\frac{3}{2})(\nu+l+\frac{1}{2})]^{1/2}, \\ \langle \nu-2, l+2 | r^2 | \nu, l \rangle &= [(\nu-1)(\nu-2)]^{1/2}, \\ \langle \nu+2, l-2 | r^2 | \nu, l \rangle &= [\nu(\nu+1)]^{1/2}. \end{aligned} \quad (14)$$

3. EIGENFUNCTIONS FOR THE DEFORMED SAXON-WOODS POTENTIAL

To simplify the calculation of the single-particle eigenfunctions for a deformed-rotating and vibrating Saxon-Woods potential it is assumed that the wave func-

tion can be separated into collective and single-particle constituents to a first approximation. The collective part is divided into rotational and vibrational eigenfunctions. The eigenfunction can then be written in the form:¹⁴

$$|IMK; N\Omega; \text{vib}\rangle = [\hat{I}/(16\pi^2)]^{1/2} \times [D^I_{MK} \chi_\Omega + (-)^{I-\frac{1}{2}} \Pi_\chi D^I_{M-K} \chi_{-\Omega}] \Phi_{\text{vib}}. \quad (15)$$

Here I is the quantum number of the total angular momentum. The symbol K is its projection in the intrinsic system. The intrinsic system is defined by the symmetry axes of the deformed potential. The Greek capital Ω is the projection of the single-particle angular momentum j in the intrinsic system.

The symbol Π_χ is the parity of the intrinsic single-particle function χ_Ω . For the ground-state rotational band it is $K=\Omega$.

The interaction between single-particle excitations, rotations, and vibrations gives a linear combination of functions (see Eq. 15). These interactions have been studied in detail by Faessler.¹⁵ Here the intrinsic particle function χ_Ω is calculated by expanding in the spherical-basis functions of Sec. 2. First, however, the Saxon-Woods potential must be generalized for the case of deformations.

There are two ways to generalize the potential (1) for multipole-vibrations or deformations. Method A, which can be used for any potential, assumes that the equipotential surfaces are deformed.

$$r = r_1 g(\theta, \phi) = r_1 (1 - \sum_{\lambda\mu} \alpha_{\lambda\mu}^\dagger \alpha_{\lambda\mu} / (4\pi) + \sum_{\lambda\mu} \alpha_{\lambda\mu} V_{\lambda\mu}). \quad (16)$$

One must replace the variable r in Eq. (1) by $r/g(\theta, \phi)$. The term $-\sum_{\lambda\mu} \alpha_{\lambda\mu}^\dagger \alpha_{\lambda\mu} / (4\pi)$ guarantees volume conservation to second order in the deformation param-

¹⁴ A. Bohr, Kgl. Danske Videnskab. Selskab, Mat. Fys. Medd. 26, No. 14 (1952).

¹⁵ A. Faessler, Nucl. Phys. 59, 177 (1964).

eters. For numerical convenience the potential is expanded in powers of $f(\theta, \phi) - 1$

$$V_A(r/g(\theta, \phi)) = \frac{\partial V}{\partial g} \Big|_{g=1} [g(\theta, \phi) - 1] + \frac{1}{2} \frac{\partial^2 V}{\partial g^2} \Big|_{g=1} [g(\theta, \phi) - 1]^2 + \dots \quad (17)$$

By inserting $g(\theta, \phi)$ of Eq. (16) into the potential (17), one gets for the deformed part of the potential

$$V_A(r, \alpha_{\lambda\mu}, \theta, \phi) = \alpha_{\lambda\mu} Y_{\lambda\mu}(\theta, \phi) \times V_0 \frac{r}{a_0} f'(y) - V_0 \frac{r}{a_0} \left[\alpha_{\lambda\mu}^\dagger \alpha_{\lambda\mu} f'(y) / 4\pi + \alpha_{\lambda\mu} Y_{\lambda\mu}(\theta, \phi) \times \alpha_{\lambda\mu} Y_{\lambda\mu}(\theta, \phi) \left(f'(y) + \frac{1}{2} \frac{r}{a_0} f''(y) \right) \right] + \dots, \quad (18)$$

where $y = (r - R_0)/a_0$ and

$$\begin{aligned} f(y) &= (1 + e^y)^{-1}, \\ f'(y) &= -e^y (1 + e^y)^{-2}, \\ f''(y) &= e^y (1 + e^y)^{-2} [2e^y (1 + e^y)^{-1} - 1]. \end{aligned} \quad (19)$$

In Eq. (18) the convention is used to sum over all double subscripts.

It is also possible to derive a deformed potential from a spherical one by a method which is not very

general but is very convenient for the Saxon-Woods shape. This is denoted as method B. The nuclear radius, R_0 , is replaced in B, in Eq. (1) by

$$R = R_0 \left[1 - \sum_{\lambda\mu} \alpha_{\lambda\mu}^\dagger \alpha_{\lambda\mu} / (4\pi) + \sum_{\lambda\mu} \alpha_{\lambda\mu} \times Y_{\lambda\mu}(\theta, \phi) \right]. \quad (20)$$

Instead of Eq. (18) this procedure leads to the following expression:

$$V_B(r, \alpha_{\lambda\mu}, \theta, \phi) = \alpha_{\lambda\mu} Y_{\lambda\mu}(\theta, \phi) V_0 \frac{R_0}{a_0} f'(y) - V_0 \frac{R_0}{a_0} \left[\alpha_{\lambda\mu}^\dagger \alpha_{\lambda\mu} \frac{f'(y)}{(4\pi)} + \frac{1}{2} (R_0/a_0) \alpha_{\lambda\mu} Y_{\lambda\mu}(\theta, \phi) \times \alpha_{\lambda\mu} Y_{\lambda\mu}(\theta, \phi) f''(y) \right]. \quad (21)$$

The main difference between methods A and B is that in method B one obtains the constant factor R_0 and R_0^2 instead of the variable r and r^2 .

For an axially symmetric deformed nucleus the equation for the equal-mass surfaces in method A [Eq. (16)] becomes

$$r = r_1 \left[1 - \sum_{\lambda} \beta_{\lambda 0}^2 / (4\pi) + \sum_{\lambda} \beta_{\lambda 0} Y_{\lambda 0}(\theta) \right]. \quad (22)$$

Correspondingly, in method B the nuclear surface is

$$R = R_0 \left[1 - \sum_{\lambda} \beta_{\lambda 0}^2 / (4\pi) + \sum_{\lambda} \beta_{\lambda 0} Y_{\lambda 0}(\theta) \right]. \quad (23)$$

Using Eqs. (22) and (23) the deformed potential of a symmetric nucleus is given in Eqs. (24) and (25) for methods A and B, respectively:

$$V_A(r, \beta_{\lambda 0}, \theta) = \beta_{\lambda 0} Y_{\lambda 0}(\theta) V_0 \frac{r}{a_0} f'(y) - V_0 \frac{r}{a_0} \beta_{\lambda 0}^2 \left[\frac{f'(y)}{(4\pi)} + Y_{\lambda 0}^2(\theta) \left(f'(y) + \frac{1}{2} \frac{r}{a_0} f''(y) \right) \right], \quad (24)$$

$$V_B(r, \beta_{\lambda 0}, \theta) = \beta_{\lambda 0} Y_{\lambda 0}(\theta) V_0 \frac{R_0}{a_0} f'(y) - V_0 \frac{R_0}{a_0} \beta_{\lambda 0}^2 \left[\frac{f'(y)}{(4\pi)} + \frac{1}{2} \frac{R_0}{a_0} Y_{\lambda 0}^2(\theta) f''(y) \right], \quad (25)$$

where $y = (r - R_0)/a_0$ and $f'(y)$ and $f''(y)$ are given in Eq. (19).

The deformation parameter β_{20} is related to the parameters used in the paper of Nilsson³ by the equations

$$\beta \approx 1.05\delta [1 + 0.51 - O(\delta^2)], \quad \delta \approx 0.95\beta [1 - 0.48\beta + O(\beta^2)], \quad \eta \approx (\delta/\kappa) [1 + (2/9)\delta^2 + \dots]. \quad (26)$$

One can now restrict the equations for symmetric quadrupole deformations $\beta_{20} = \beta_0$. The spherical Hamiltonian is

$$H_0 = \frac{p^2}{2m} + V(l). \quad (27)$$

The potential $V(r)$ is defined in Eqs. (1) and (7). It contains a Thomas-type spin-orbit coupling for which the deformation (as in the Nilsson calculations) is not taken into account. The nonspherical part of the potential is

$$V_A(r, \beta_0, \theta) = \beta_0 V_0 (r/a_0) f'(y) Y_{20}(\theta) - \beta_0^2 V_0 (r/a_0) \left\{ f'(y) / (2\pi) + (r/a_0) f''(y) / (8\pi) + (2/7) (5/4\pi)^{1/2} Y_{20}(\theta) [f'(y) + \frac{1}{2} (r/a_0) f''(y)] + (6/7) (1/4\pi)^{1/2} Y_{40}(\theta) [f'(y) + \frac{1}{2} (r/a_0) f''(y)] \right\} \quad (28)$$

and

$$V_B(r, \beta_0, \theta) = \beta_0 V_0 (R_0/a_0) f'(y) Y_{20}(\theta) - \beta_0^2 V_0 (R_0/a_0) \left[f'(y) / (4\pi) + (R_0/a_0) f''(y) / (8\pi) + (1/7) (5/4\pi)^{1/2} (R_0/a_0) f''(y) Y_{20}(\theta) + (3/7) (1/4\pi)^{1/2} (R_0/a_0) f''(y) Y_{40}(\theta) \right]. \quad (29)$$

TABLE IV. The mixing coefficients for the $\frac{1}{2}-[510]$ neutron state are compared for method B (Table VII), and method A, the Nilsson model, and the experimental value from the (d,p) reaction for the nucleus ^{177}Yb $\beta \approx 0.25$. The deformation for the theoretical values is $\beta = 0.2$, which is the experimental deformation in ^{183}W .

	$C_{3p1/2}$	$C_{3p3/2}$	$C_{2f5/2}$	$C_{2f7/2}$	$C_{1h9/2}$	$C_{1h11/2}$	$a_{[510]}$
B	0.102	0.651	0.569	-0.349	-0.337	0.079	0.18
A	0.092	0.654	0.571	-0.352	-0.329	0.078	0.14
Nilsson	-0.058	0.675	0.569	-0.371	-0.268	0.079	-0.17
Experiment	± 0.13	± 0.58	± 0.63	± 0.41			0.22

The product of the two spherical harmonics is expanded into a Clebsch-Gordan series.

The volume conservation is incorporated in the perturbation Hamiltonian. Nilsson has included it in the spherical part by letting the unperturbed potential depend on the deformation. This can also be accomplished by introducing a deformation-dependent radius $R = R_0(1 - \beta_0^2/4\pi)$. If one has analytic solutions for the spherical potential, then this method is feasible. But for the Saxon-Woods potential it would mean the numerical recalculation of the basic functions for each deformation. Following Nilsson,³ we diagonalize the matrix:

$$\langle \nu' j' l' \Omega | H_A | \nu j l \Omega \rangle = E_{\nu j l} \delta_{\nu' j' l' \nu j l} + \langle \nu' j' l' \Omega | V_A | \nu j l \Omega \rangle, \quad (30)$$

or

$$\langle \nu' j' l' \Omega | H_B | \nu j l \Omega \rangle = E_{\nu j l} \delta_{\nu' j' l' \nu j l} + \langle \nu' j' l' \Omega | V_B | \nu j l \Omega \rangle, \quad (31)$$

where the vectors $|\nu j l \Omega\rangle$ are confined to a single $N = 2\nu + l - 2$ shell. Here, to be sure, the vectors $|\nu j l \Omega\rangle$ are Saxon-Woods eigenfunctions, and the quantities V_A and V_B are given in (28) and (29).

The results of method B are given in Table VII at the end of this paper for rare-earth nuclei. The mixing coefficients for the spherical basis $|\nu j l \Omega\rangle$ are tabulated for the mass number $A = 185$ and the deformations $\beta = 0.1, 0.2, 0.3, 0.4$. The optical model fits for protons of Bjorklund and Fernbach⁸ and of Perey⁹ have been utilized as the starting point for the choice of the parameters. The values $r_0 = 1.25$ F, $C_0 = 10$ MeV, and $a_0 = 0.64$ F have been used for the neutrons as in the optical model. Because the Coulomb interaction has been neglected, a steeper well has been utilized for the protons. For the same reason the well depth for the proton $V_0 = 35.24$ MeV is less than the neutron well depth $V_0 = 46.33$ MeV by about the Coulomb interaction of one proton with the nucleus. Both have been fitted utilizing the binding energy of the last particle in the appropriate spherical nuclei (see Table I). Unfortunately, in this case it is not possible as in the case of an oscillator potential^{8,16} to perform the calculation independent of the mass number. (This is obvious because of the fact that for different masses the same state can be bound and unbound.) Therefore, the tabulated coefficients are only correct for the mass $A = 185$. However,

¹⁶ B. R. Mottelson and S. G. Nilsson, Kgl. Danske Videnskab. Selskab, Mat. Fys. Skrifter I, No. 8 (1959).

Table III indicates that variation of the coefficients C_{jl} with the mass number is small.

In Table IV the neutron eigenfunction $\frac{1}{2}-[510]$ (where the classification of the state utilizes the asymptotic quantum numbers³ $\Omega\pi[Nn_z\Lambda]$) using methods A and B is compared with that using the Nilsson functions for $\beta = 0.2$. Although the differences in the mixing coefficients are small, the decoupling parameter a for [510] is changed by 22% in going from method B to method A. The Nilsson function (shown in row 3) gives the wrong sign for the decoupling parameter.¹⁶ The explanation lies in the coefficient $c_{1h9/2}$, which is too small. In the last row the experimental mixing coefficients are given.¹⁷ To extract the coefficients from the experimental data, a truncated oscillator potential has been utilized. They have been measured by the (d,p) reaction in the nucleus Yb¹⁷⁷, which has a deformation of about $\beta = 0.25$. The experimental values for the decoupling parameter of the $\frac{1}{2}-[510]$ rotational band show a tendency to decrease¹⁸ as the mass number increases. This calculation reproduces this effect as Fig. 4 shows, although it cannot fully account for the diminution. The augmentation of the mass number enlarges the binding energy of the

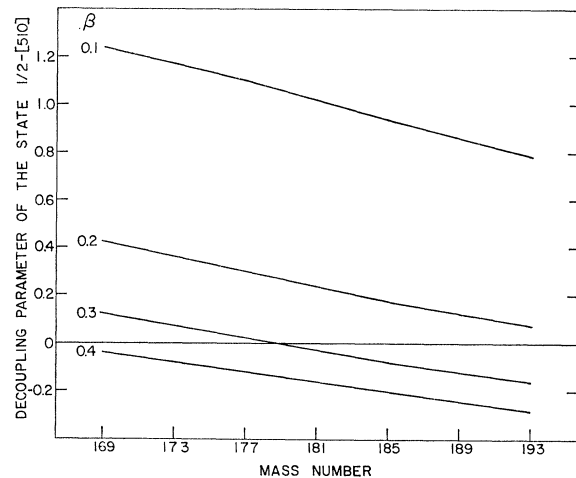


FIG. 4. Dependence of the decoupling parameter of the $\frac{1}{2}-[510]$ band for the deformations $\beta = 0.1, 0.2, 0.3, 0.4$ on the mass number A . The decrease of this value with increasing mass is observed experimentally.

¹⁷ M. N. Vergnes and R. K. Sheline, Phys. Rev. **132**, 1736 (1963).

¹⁸ B. Harmatz, T. H. Handley, and J. W. Mihelich, Phys. Rev. **128**, 1186 (1962).

TABLE V. The decoupling parameters for the rare-earth region are tabulated. The first column lists the state for which the function has the largest mixing coefficient at $\beta=0.1$. Column two gives the decoupling parameter for the spherical state, $[a_0 = (-)^{j-1/2} \times (j+1/2)]$. Columns three to six give the decoupling parameter according to the Saxon-Woods potential. The decoupling parameter for infinite deformation is calculated with the asymptotic functions $[a_\infty = (-)^N \delta_{\Lambda,0}]$. In the last column the asymptotic quantum numbers $\Omega\pi[Nn_z\Lambda]$ are given.

β	0	0.1	0.2	0.3	0.4	∞	$\Omega\pi[Nn_z\Lambda]$
γ_{lj}			For protons				
$1g_{7/2}$	-4.00	-2.13	-0.68	-0.25	0.06	0	$\frac{1}{2} + [431]$
$2d_{5/2}$	3.00	1.07	-0.38	-0.67	-0.71	1.00	$\frac{3}{2} + [420]$
$2d_{3/2}$	-2.00	-0.65	-0.70	-0.69	-0.68	0	$\frac{3}{2} + [411]$
$3s_{1/2}$	1.00	-0.21	0.02	0.14	0.22	1.00	$\frac{1}{2} + [400]$
$1h_{11/2}$	-6.00	-5.93	-5.74	-5.44	-5.06	-1.00	$\frac{1}{2} - [550]$
$2f_{7/2}$	-4.00	-3.82	-3.66	-3.67	-3.78	0	$\frac{1}{2} - [541]$
ν_{lj}			For neutrons				
$2f_{7/2}$	-4.00	-3.43	-1.59	-0.62	-0.39	0	$\frac{1}{2} - [541]$
$1h_{9/2}$	5.00	4.41	2.35	1.01	0.22	-1.00	$\frac{1}{2} - [530]$
$3p_{3/2}$	-2.00	-0.26	0.51	0.73	0.79	0	$\frac{3}{2} - [521]$
$2f_{5/2}$	3.00	0.94	0.18	-0.07	-0.21	-1.00	$\frac{3}{2} - [510]$
$3p_{1/2}$	1.00	1.25	1.20	1.15	1.13	0	$\frac{3}{2} - [501]$
$1i_{13/2}$	7.00	6.92	6.66	6.25	5.74	1.00	$\frac{1}{2} + [660]$
$2g_{9/2}$	5.00	4.73	4.41	4.32	4.37	0	$\frac{1}{2} + [651]$

state and therefore makes the difference between the oscillator and the Saxon-Woods functions smaller.

In Table V the decoupling parameters for the rare earth region are tabulated. The most striking change compared with the values of Mottelson and Nilsson¹⁶ (p. 84) involve the $\frac{1}{2} - [510]$ orbital mentioned above. The calculations presented here move in the right direction in improving the agreement between theory and the experimental results, especially in the W isotopes.

Figures 5 and 6 show the proton and the neutron levels versus the deformation for the mass region

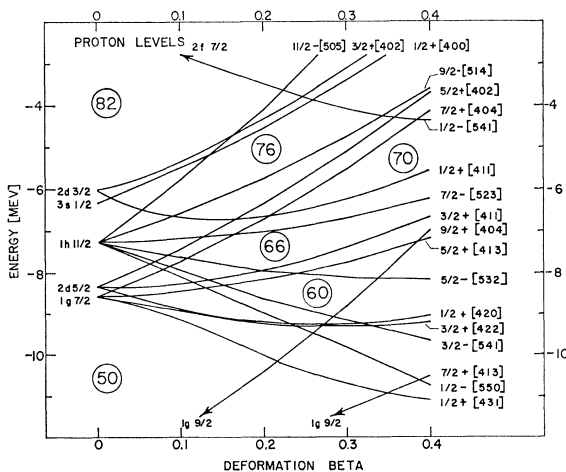


FIG. 5. The single-particle proton levels versus the deformation $\beta \approx 1.05\delta \approx 1.05\eta\kappa$ are shown for the Saxon-Woods potential for the mass number 185 in the rare-earth region. The well depth is $V_0 = 35.24$ MeV, the radius parameter $r_0 = 1.25$ F, the diffuseness parameter $a_0 = 0.52$ F, and the spin-orbit constant $C_0 = 10$ MeV.

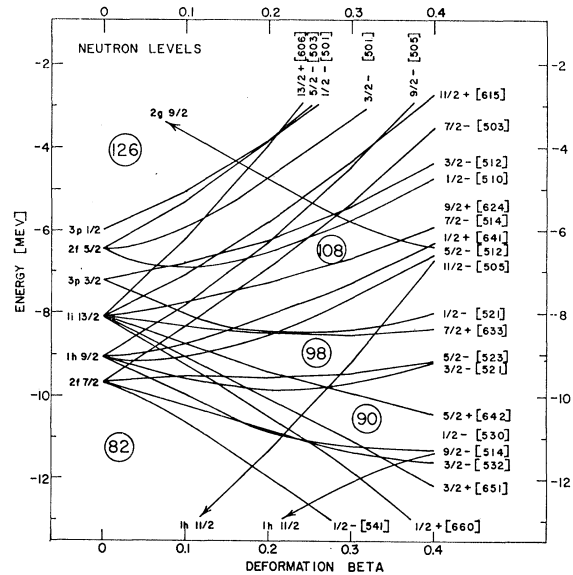


FIG. 6. The single-particle neutron levels versus the deformation $\beta \approx 1.05\delta \approx 1.05\eta\kappa$ are shown for the Saxon-Woods potential for the mass number $A = 185$ in the rare-earth region. The well depth is $V_0 = 46.33$ MeV, the radius constant $r_0 = 1.25$ F, the diffuseness parameter $a_0 = 0.64$ F, and the spin-orbit constant $C_0 = 10$ MeV.

$150 \leq A \leq 190$. For the proton orbits the state $\frac{1}{2} + [400]$ lies lower than the $\frac{3}{2} + [402]$, in contrast to the calculations of Nilsson. Until now there has been no definite experimental evidence for either of the two sequences. If the assignment of the $K = \frac{1}{2} +$ band in Re^{185} at 646 keV as the $\frac{1}{2} + [400]$ band is correct, this favors the sequence of orbitals of this calculation. It seems probable, however,¹⁵ that this band is the $K = \Omega - 2 \gamma$ vibrational band built on the intrinsic state $\frac{5}{2} + [402]$.

The neutron orbits in Fig. 6 show the right sequence of the $\frac{7}{2} + [633]$ and the $\frac{1}{2} - [521]$ states. These are the ground state for the 99th and 101st neutrons. In the original Nilsson¹⁶ calculation these two single-particle levels have the wrong order of succession for the experimental deformation. Probably, however, they could be reversed without seriously affecting the otherwise good agreement.

Thus the present experimental evidence on orbital sequences in the rare-earth nuclei does not allow a clear choice between these calculations and those of Mottelson and Nilsson.

4. ELECTROMAGNETIC TRANSITION PROBABILITIES IN DEFORMED NUCLEI

As successful as the Nilsson model is in explaining the energy sequence and the intrinsic nature of the states in deformed nuclei, the calculations of absolute values of electromagnetic transition probabilities have not been satisfactory. A compilation of the hindrance factors derived from the Nilsson model $F_n = P_{\text{Nilsson}}/P_{\text{experiment}}$

is given by Loebner.¹⁹ The $E1$ transitions fall into two groups with $\Delta K=0$ and $\Delta K=1$. The former agree reasonably well with the experimental results, while the latter are larger than the Nilsson values by a factor up to 10^3 . If one takes into account the short-range correlations of the nucleons the electric γ -ray transitions are reduced by a factor^{20,21}

$$R^2 = (u_f u_i - v_f v_i)^2 \approx \frac{(E_i - E_f)^2 \left[\left(\frac{E_i + E_f}{E_i - E_f} \right)^2 - 1 \right]}{4E_i E_f} \approx \frac{1}{2} (E_i - E_f) / (E_i - E_f + \Delta). \quad (32)$$

Here the E 's are the quasiparticle energies and Δ is the half-energy gap. The gap is given by the odd-even mass differences in the binding energy.

$$\Delta = |P_n(Z, N)| = \left| \frac{1}{4} [2S_n(Z, N) - S_n(Z, N+1) - S_n(Z, N-1)] \right| \quad (33)$$

for odd-neutron nuclei and

$$\Delta = |P_n(Z, N)| = \left| \frac{1}{4} [2S_p(Z, N) - S_p(Z+1, N) - S_p(Z-1, N)] \right| \quad (34)$$

for odd-proton nuclei. The neutron separation energies S_n and the proton separation energies S_p are tabulated by Yamada and Matumoto²² and by Mattauch, Thiele and Wapstra.²³ For the rare-earth nuclei, one finds Δ in Ref. 24. In Eq. (32) the difference of the quasi-particle energies $E_i - E_f$ is the bandhead-to-bandhead transition energy. The final simplification in Eq. (32) is only possible for single-particle energies $\epsilon_f \ll \Delta$. Vergnes and Rasmussen²⁵ and also Monsonogo and Piepenbring²⁶ have shown that with the reduction factor R^2 the $\Delta K=1$, $E1$ transitions agree fairly well with the experimental results. Then, however, the $\Delta K=0$, $E1$ transitions are too small. The solution of the problem²⁷ seems to lie in a mixing of the initial state and the octupole vibration of the final state, and vice versa. This mixing enhances only the $\Delta K=0$, $E1$ transitions because the octupole-vibrational band with $\Delta K=0$, respectively, to the ground-state rotational band, is expected to be situated much lower in energy and to have a greater collective strength than the $\Delta K=1$, 2, and 3 bands.

¹⁹ K. E. G. Loebner, thesis, Amsterdam, 1965 (unpublished).

²⁰ L. S. Kisslinger and R. A. Sorensen, Kgl. Danske Videnskab. Selskab, Mat. Fys. Medd. **32**, No. 9 (1960).

²¹ H. Ikegami and T. Udagawa, Phys. Rev. **133**, B1388 (1964).

²² M. Yamada and Z. Matumoto, J. Phys. Soc. Japan **16**, 1497 (1961).

²³ T. Mattauch, W. Thiele, and A. H. Wapstra, Nucl. Phys. **67**, 1 (1965).

²⁴ S. G. Nilsson and O. Prior, Kgl. Danske Videnskab. Selskab, Mat. Fys. Medd. **32**, No. 16 (1960).

²⁵ M. N. Vergnes and F. O. Rasmussen, Nucl. Phys. **62**, 233 (1965).

²⁶ G. Monsonogo and R. Piepenbring, Nucl. Phys. **58**, 593 (1964).

²⁷ A. Faessler, T. Udagawa, and R. K. Sheline (to be published).

Although only a few absolute $E2$ -transitions have been measured, the available data show two groups,¹⁹ the $E2$ $\Delta K=1$ and the $E2$ $\Delta K=2$ transitions. The $E2$ $\Delta K=1$ transitions are enhanced by a factor 10^2 to 10^5 compared with the Nilsson model. Faessler^{15,28} has shown that these discrepancies can be removed by considering the Coriolis interaction between the particle and the collective rotation. But in Refs. 15 and 28 it is also shown that the rotation-vibration interaction enhances this effect by the factor

$$f = \left[1 + \frac{9 \hbar^2}{2 J_0 E_\beta} + \frac{3 \hbar^2}{2 J_0 E_\gamma} \right]^2, \quad (35)$$

where J_0 is the moment of inertia and E_β and E_γ are the β and γ vibrational energies, respectively. This factor is about 1.3 for the Sm and the Os regions. The collective enhanced transition probability is not reduced by the pairing interaction because the Coriolis force is positive under time reversal.

The $\Delta K=2$ $E2$ transitions are enhanced by the rotation-vibration and the vibration-particle¹⁵ interactions and reduced by the pairing reduction factor. But because the phenomenological interactions give only a mixing of final and initial states in second-order perturbation theory, it does not outweigh the pairing reduction factor.

For electric-octupole transitions the absolute values are known with certainty only for the $\Delta K=3$ transitions. In the other cases the mixing ratio $E3/M2$ is uncertain. Loebner¹⁹ reports hindrance factors F_N between 3 and 6 for these transitions.

The $M1$ -transition probabilities depend strongly^{15,19} on the collective g_R factor. It is possible to fit the transition probabilities in most cases with reasonable values g_R . Loebner,¹⁹ however, calls attention to two cases (in ${}_{64}^{155}\text{Gd}$, $\frac{5}{2} + [642] \rightarrow \frac{3}{2} + [651]$, $F_N \approx 200$; and in ${}_{73}^{181}\text{Ta}$, $\frac{5}{2} + [402] \rightarrow \frac{7}{2} + [404]$, $F_N \geq 1200$) which still demand explanation. In Table VI the r^2 matrix elements with Saxon-Woods functions (first row) and with oscillator functions (second row) are compared. The oscillator matrix elements are in many cases smaller than the Saxon-Woods matrix elements. With our choice of parameters, the oscillator potential (particularly in the region of 6 MeV binding energy) lies outside the Saxon-Woods potential (Fig. 1). This compresses the Saxon-Woods functions more than the oscillator functions. For small binding energies and more than one node the Saxon-Woods functions have a greater probability of being outside of the nucleus and the r^2 matrix element is larger by a factor of up to 2.5 in the case of $\langle 4s_{1/2} | r^2 | 4s_{1/2} \rangle$. The $E2$ -transition probability between the $4s_{1/2}$ and the $3d_{5/2}$ states of Fig. 3 would be enhanced by a factor 2.85 according to Table VI. This effect is very important in light nuclei where the excited nucleons often have only

²⁸ A. Faessler, contribution to *Internal Conversion Processes* (Academic Press Inc., New York, to be published).

TABLE VI. The $\langle |r^2| \rangle$ matrix element is tabulated for the rare-earth region. The first row gives the Saxon-Woods value and the second the oscillator value both in units of $[\hbar/m\omega]$ with $\hbar\omega = 41/185^{1/3}$ MeV.

Neutrons	$3s_{1/2}$	$2d_{5/2}$	$2d_{3/2}$	$1g_{9/2}$	$1g_{7/2}$	$3p_{3/2}$	$2f_{7/2}$	$1h_{11/2}$	$1h_{9/2}$	Protons	
$3p_{3/2}$	6.158 6.500	5.594 5.500	5.221 5.292	5.067 5.292	3.503 3.742	2.572 3.742	5.833 5.278	6.102 5.830	4.347 4.801	3.491 4.801	$3s_{1/2}$
$3p_{1/2}$	6.233 6.500	6.332 6.500	5.462 5.500	5.402 5.500	3.919 4.243	3.018 4.243	4.514 4.514	5.778 5.593	4.688 5.184	3.863 5.184	$2d_{5/2}$
$2f_{7/2}$	5.352 6.000	5.499 6.000	5.875 6.500	5.426 5.500	4.271 4.243	3.434 4.243	4.355 4.514	5.567 5.593	4.982 5.184	4.251 5.184	$2d_{3/2}$
$2f_{5/2}$	5.151 6.000	5.337 6.000	5.828 6.500	5.884 6.500	6.201 5.500	5.739 5.500	2.277 2.579	3.186 3.439	6.473 5.865	6.145 5.865	$1g_{9/2}$
$1h_{11/2}$	3.043 3.838	3.277 3.838	3.768 4.690	4.226 4.690	6.291 6.500	5.468 5.500	1.489 2.579	2.159 3.439	5.856 5.865	5.728 5.865	$1g_{7/2}$
$1h_{9/2}$	2.213 3.838	2.446 3.838	2.921 4.690	3.430 4.690	5.906 6.500	5.668 6.500	12.911 6.500	7.317 6.000	3.268 3.838	2.779 3.838	$3p_{3/2}$
$4s_{1/2}$	5.595 5.700	5.809 5.700	3.619 4.374	3.599 4.374	1.446 2.222	1.035 2.222	18.523 7.500	7.113 6.500	4.185 4.690	3.264 4.690	$2f_{7/2}$
$3d_{5/2}$	6.491 6.299	6.608 6.299	4.542 4.985	4.355 4.985	1.965 2.592	1.327 2.592	12.380 7.348	10.510 7.500	6.896 6.500	6.415 6.500	$1h_{11/2}$
$2g_{9/2}$	6.416 6.782	6.531 6.782	6.167 6.599	5.971 6.599	3.039 3.751	2.122 3.751	6.270 6.155	6.860 6.633	7.254 7.500	6.169 6.500	$1h_{9/2}$
$1i_{13/2}$	3.906 5.033	4.143 5.033	4.557 5.751	4.962 5.751	6.535 6.867	6.022 6.867	2.243 3.476	2.885 3.903	4.011 5.099	6.917 7.500	
Neutrons	$3p_{3/2}$	$3p_{1/2}$	$2f_{7/2}$	$2f_{5/2}$	$1h_{11/2}$	$1h_{9/2}$	$4s_{1/2}$	$3d_{5/2}$	$2g_{9/2}$	$1i_{13/2}$	

small binding energies. An enlargement of a transition probability between such states may not indicate a collective nature. (Strocke *et al.*²⁹ give also an extensive tabulation of this matrix element in connection with the Bohr-Weisskopf effect.)

5. CONCLUSION

The Schrödinger equation for nucleons with a Saxon-Woods potential and Thomas-type spin-orbit coupling has been solved numerically for the mass number $A=185$ and for the $N=4$ and 5 proton shells and the $N=5$ and 6 neutron shells. The overlap integral with the corresponding oscillator function is always greater than 0.92 for states with a binding energy of 2 MeV or greater. The most serious discrepancy is the neutron $4s_{1/2}$ state with binding energy of only 0.41 MeV and an overlap integral of 0.80. To get an analytic expression for the Saxon-Woods functions they have been expanded in Table II into oscillator functions. The first 6 coefficients represent the wave function to better than 99% for binding energies of 2 MeV and greater. For small binding energies, however, the convergence is very slow, a big exponential tail not being easily represented by Gaussian slopes. In the case of the $4s_{1/2}$ state the first 6 coefficients represent 73% and the first 10 coefficients 88% of the whole Saxon-Woods function.

In Sec. 3 the Schrödinger equation for an axially symmetric quadrupole deformed potential with Saxon-Woods shape and a Thomas type spin-orbit coupling has been solved. The single particle energies reproduce the experimental level sequence including the orbitals

$\frac{7}{2}+ [633]$ and $\frac{1}{2}- [521]$. Furthermore, this calculation gives the right value for the decoupling parameter in the $\frac{1}{2}- [510]$ rotational band. It explains also the decrease of this decoupling parameter with increasing mass number which is observed experimentally. The mixing coefficients for the rare-earth region are tabulated in Table VII. The application of these calculations to gamma transition probabilities has been considered in Sec. 4. Expressions for the transition probabilities in the (jK) representation are given in the Appendix.

The transition matrix elements depend strongly on the width of the well near the binding energy. For positive powers of r the matrix elements are greater, the greater the width. The difference increases with the power of r . The Saxon-Woods r^2 matrix elements deviate as much as 60% from the corresponding oscillator matrix elements. For matrix elements between states with a small binding energy, (<2 MeV) and more than one node Saxon-Woods matrix element is always larger than the oscillator matrix element. This is especially important in light nuclei. *Note added in proof.* After finishing these calculations, the authors were informed that similar calculations have been done and are being done by Rost *et al.*³⁰ and by Tamura.³¹ Davies, Krieger, and Baranger³² did Hartree-Fock calculations employing an oscillator basis. They found the same fast conversion of the Hartree-Fock functions for an expansion into an oscillator basis as it is reported here for Saxon-Woods functions.

³⁰ E. Rost and G. E. Brown, Bull. Am. Phys. Soc. **10**, 487 (1965); E. Rost, Princeton University Report No. PUC-937-66-202 (unpublished).

³¹ T. Tamura (unpublished).

³² T. R. Davies, S. J. Krieger, and M. Baranger, Nucl. Phys. (to be published).

²⁹ M. H. Stroke, R. J. Blin-Stoyle, and V. Jaccarino, Phys. Rev. **123**, 1326 (1961).

TABLE VII. The eigenfunctions for a deformed Saxon-Woods potential are tabulated. The expansion coefficients C_{jl} for the spherical Saxon-Woods function $|\nu j l K\rangle$ of Eq. (2) are listed for the deformations $\beta=0.1, 0.2, 0.3, 0.4$. The proton coefficients are calculated for the $N(=2\nu+l-2)=4$ and the $N=5$ shells. The parameters are: $A=185$; $r_0=1.25$ F; $a_0=0.52$ F; $V_0=35.24$ MeV; $C_0=10$ MeV. The free states $3p_{1/2}$ and $2f_{5/2}$ have been dropped. The neutron coefficients are calculated for the $N=5$ and $N=6$ shells. The parameters are: $A=185$; $r_0=1.25$ F; $a_0=0.64$ F; $V_0=46.33$ MeV; $C_0=10$ MeV. The free states $2g_{7/2}$ and $3d_{3/2}$ have been dropped. The first column lists the quantum numbers ν, j, l .

Proton mixing coefficients									
$N=4 \quad \Omega=1/2$									
		$[Nn_z\Delta]=[440]$				$[Nn_z\Delta]=[431]$			
β		0.1	0.2	0.3	0.4	0.1	0.2	0.3	0.4
Energy [MeV]		-13.6686	-14.2884	-14.7626	-15.0730	-9.2088	-10.0050	-10.6622	-11.0810
ν	$j \quad l$								
1	9/2 4	0.9817	0.9358	0.8704	0.7879	0.1013	0.2342	0.3364	0.4248
1	7/2 4	-0.0109	-0.0206	-0.0281	-0.0324	0.8150	0.5991	0.4934	0.4212
2	5/2 2	0.1889	0.3446	0.4716	0.5747	0.4500	0.4980	0.4138	0.3085
2	3/2 2	-0.0058	-0.0234	-0.0505	-0.0849	0.2917	0.4480	0.5254	0.5682
3	1/2 0	0.0198	0.0667	0.1292	0.2017	-0.1947	-0.3708	-0.4429	-0.4734
$[Nn_z\Delta]=[420]$									
β		0.1	0.2	0.3	0.4	0.1	0.2	0.3	0.4
Energy [MeV]		-8.8937	-9.2067	-9.2558	-9.0334	-6.6935	-6.6309	-6.2243	-5.5706
ν	$j \quad l$								
1	9/2 4	-0.1540	-0.2296	-0.2971	-0.3581	-0.0434	-0.1170	-0.1826	-0.2376
1	7/2 4	0.5130	0.6761	0.6971	0.6943	-0.2288	-0.3819	-0.4677	-0.5261
2	5/2 2	0.8033	0.6160	0.5260	0.4552	0.2953	0.4267	0.4749	0.4888
2	3/2 2	0.0316	0.1474	0.2182	0.2735	0.7240	0.6804	0.6266	0.5781
3	1/2 0	0.2583	0.2982	0.3185	0.3282	-0.5783	-0.4421	-0.3602	-0.3059
$[Nn_z\Delta]=[400]$									
β		0.1	0.2	0.3	0.4				
Energy [MeV]		-5.5090	-4.5475	-3.4043	-2.1077				
ν	$j \quad l$								
1	9/2 4	0.0200	0.0543	0.0877	0.1191				
1	7/2 4	-0.1415	-0.1940	-0.2258	-0.2503				
2	5/2 2	-0.1711	-0.2677	-0.3227	-0.3583				
2	3/2 2	0.6243	0.5604	0.5303	0.5107				
3	1/2 0	0.7487	0.7574	0.7457	0.7307				
$N=4 \quad \Omega=3/2$									
		$[Nn_z\Delta]=[431]$				$[Nn_z\Delta]=[422]$			
β		0.1	0.2	0.3	0.4	0.1	0.2	0.3	0.4
Energy [MeV]		-13.4790	-13.8923	-14.1411	-14.1944	-8.9368	-9.2045	-9.2915	-9.1947
ν	$j \quad l$								
1	9/2 4	0.9868	0.9575	0.9217	0.8831	0.0841	0.1608	0.2164	0.2576
1	7/2 4	-0.0303	-0.0547	-0.0706	-0.0782	0.9169	0.8725	0.8445	0.8212
2	5/2 2	0.1588	0.2820	0.3788	0.4582	-0.3371	-0.3492	-0.3257	-0.2994
2	3/2 2	-0.0084	-0.0258	-0.0450	-0.0635	0.1964	0.3016	0.3660	0.4118
$[Nn_z\Delta]=[411]$									
β		0.1	0.2	0.3	0.4	0.1	0.2	0.3	0.4
Energy [MeV]		-8.2629	-7.9298	-7.3867	-6.6434	-5.3129	-4.3121	-3.1047	-1.7148
ν	$j \quad l$								
1	9/2 4	-0.1371	-0.2347	-0.3218	-0.3782	-0.0178	-0.0472	-0.0764	-0.1035
1	7/2 4	0.3647	0.4227	0.4464	0.4649	-0.1593	-0.2391	-0.2874	-0.3215
2	5/2 2	0.9185	0.8708	0.8318	0.7923	0.1322	0.2006	0.2420	0.2695
2	3/2 2	-0.0672	-0.0892	-0.1049	-0.1145	0.9782	0.9489	0.9236	0.9018
$N=4 \quad \Omega=5/2$									
		$[Nn_z\Delta]=[422]$				$[Nn_z\Delta]=[413]$			
β		0.1	0.2	0.3	0.4	0.1	0.2	0.3	0.4
Energy [MeV]		-13.1044	-13.1396	-13.0420	-12.7972	-8.4431	-8.1666	-7.7390	-7.1693
ν	$j \quad l$								
1	9/2 4	0.9936	0.9798	0.9632	0.9456	0.0671	0.1242	0.1687	0.2039
1	7/2 4	-0.0445	-0.0829	-0.1143	-0.1397	0.9719	0.9656	0.9618	0.9582
2	5/2 2	0.1041	0.1820	0.2433	0.2937	-0.2254	-0.2286	-0.2157	-0.2006

TABLE VII (continued)

$N=4 \quad \Omega=5/2$ (continued)										
$[Nn_z\Lambda]=[402]$										
β	0.1	0.2	0.3	0.4						
Energy [MeV]	-7.4271	-6.3344	-5.0743	-3.6522						
ν	j	l								
1	9/2	4	-0.0911	-0.1568	-0.2093	-0.2535				
1	7/2	4	0.2310	0.2466	0.2488	0.2495				
2	5/2	2	0.9687	0.8563	0.9457	0.9346				
$N=4 \quad \Omega=7/2$										
$[Nn_z\Lambda]=[413]$					$[Nn_z\Lambda]=[404]$					
β	0.1	0.2	0.3	0.4	0.1	0.2	0.3	0.4		
Energy [MeV]	-12.5419	-11.9908	-11.3107	-10.5008	-7.7485	-6.7251	-5.4996	-4.0725		
ν	j	l								
1	9/2	4	0.9989	0.9959	0.9916	0.9865	0.0472	0.0905	0.1294	0.1639
1	7/2	4	-0.0472	-0.0905	-0.1294	-0.1639	0.9989	0.9959	0.9916	0.9865
$N=4 \quad \Omega=9/2$										
$[Nn_z\Lambda]=[404]$										
β	0.1	0.2	0.3	0.4						
Energy [MeV]	-11.7836	-10.3864	-8.7721	-6.9409						
ν	j	l								
1	9/2	4	1.0000	1.0000	1.0000	1.0000				
$N=5 \quad \Omega=1/2$										
$[Nn_z\Lambda]=[550]$					$[Nn_z\Lambda]=[541]$					
β	0.1	0.2	0.3	0.4	0.1	0.2	0.3	0.4		
Energy [MeV]	-8.1281	-8.9647	-9.8068	-10.7209	-2.7903	-3.4910	-4.0346	-4.3179		
ν	j	l								
1	11/2	5	0.9833	0.9373	0.8643	0.7705	-0.1765	-0.3277	-0.4631	-0.5762
1	9/2	5	-0.0057	-0.0098	-0.0120	-0.0127	-0.0218	-0.0248	-0.0227	-0.0211
2	7/2	3	0.1806	0.3404	0.4785	0.5876	0.9217	0.7868	0.6375	0.4763
3	3/2	1	0.0204	0.0748	0.1543	0.2467	0.3446	0.5224	0.6152	0.6638
$[Nn_z\Lambda]=[530]$					$[Nn_z\Lambda]=[521]$					
β	0.1	0.2	0.3	0.4	0.1	0.2	0.3	0.4		
Energy [MeV]	-1.3005	-1.4179	-1.1840	-0.5987	-0.5482	-0.3071	0.1299	0.7263		
ν	j	l								
1	11/2	5	0.0022	0.0034	0.0048	0.0065	0.0434	0.1190	0.1960	0.2726
1	9/2	5	0.9997	0.9994	0.9993	0.9992	-0.0123	-0.0201	-0.0254	-0.0326
2	7/2	3	0.0170	0.0125	0.0049	-0.0038	0.3428	-0.5147	-0.6038	-0.6541
3	3/2	1	0.0192	0.0308	0.0354	0.0402	0.9383	0.8489	0.7723	0.7049
$N=5 \quad \Omega=3/2$										
$[Nn_z\Lambda]=[541]$					$[Nn_z\Lambda]=[532]$					
β	0.1	0.2	0.3	0.4	0.1	0.2	0.3	0.4		
Energy [MeV]	-7.9701	-8.6116	-9.1690	-9.6453	-2.4276	-2.5966	-2.5562	-2.2914		
ν	j	l								
1	11/2	5	0.9865	0.9526	0.9055	0.8495	-0.1620	-0.2970	-0.4093	-0.5015
1	9/2	5	-0.0165	-0.0291	-0.0366	-0.0399	-0.0767	-0.1170	-0.1349	-0.1443
2	7/2	3	0.1626	0.2999	0.4156	0.5124	0.9582	0.8856	0.8024	0.7105
3	3/2	1	0.0124	0.0411	0.0781	0.1191	0.2282	0.3374	0.4128	0.4721
$[Nn_z\Lambda]=[521]$					$[Nn_z\Lambda]=[512]$					
β	0.1	0.2	0.3	0.4	0.1	0.2	0.3	0.4		
Energy [MeV]	-1.1611	-1.1933	-0.9356	-0.3882	-0.0153	0.5584	1.1994	1.8956		
ν	j	l								
1	11/2	5	0.0043	-0.0057	-0.0194	-0.0340	0.0243	0.0654	0.1106	0.1602
1	9/2	5	0.9968	0.9925	0.9898	0.9883	-0.0143	-0.0218	-0.0259	-0.0304
2	7/2	3	0.0733	0.1057	0.1139	0.1100	-0.2235	-0.3385	-0.4129	-0.4697
3	3/2	1	0.0313	0.0616	0.0828	0.1004	0.9743	0.9385	0.9037	0.8676

TABLE VII (continued)

$N=5 \quad \Omega=5/2$										
$[Nn_z\Delta]=[532]$				$[Nn_z\Delta]=[523]$						
β	0.1	0.2	0.3	0.4	0.1	0.2	0.3	0.4		
Energy [MeV]	-7.6579	-7.9565	-8.1288	-8.1607	-1.8724	-1.4849	-0.9706	-0.3334		
ν	j	l								
1	11/2	5	0.9913	0.9712	0.9454	0.9164	-0.1317	-0.2358	-0.3042	-0.3392
1	9/2	5	-0.0260	-0.0475	-0.0635	-0.0740	-0.1511	-0.3353	-0.5247	-0.6657
2	7/2	3	0.1293	0.2336	0.3198	0.3935	0.9797	0.9121	0.7951	0.6647
$[Nn_z\Delta]=[512]$										
β	0.1	0.2	0.3	0.4						
Energy [MeV]	-0.8651	-0.6426	-0.1590	0.5757						
ν	j	l								
1	11/2	5	0.0059	-0.0350	-0.1173	-0.2127				
1	9/2	5	0.9882	0.9409	0.8489	0.7425				
2	7/2	3	0.1532	0.3369	0.5153	0.6351				
$N=5 \quad \Omega=7/2$										
$[Nn_z\Delta]=[523]$				$[Nn_z\Delta]=[514]$						
β	0.1	0.2	0.3	0.4	0.1	0.2	0.3	0.4		
Energy [MeV]	-7.1929	-7.0075	-6.6950	-6.2486	-1.2049	-0.3426	0.4642	1.3331		
ν	j	l								
1	11/2	5	0.9961	0.9871	0.9753	0.9615	-0.0874	-0.1569	0.1960	0.2255
1	9/2	5	-0.0322	-0.0619	-0.0884	-0.1118	-0.2133	-0.5590	0.7701	0.8431
2	7/2	3	0.0824	0.1478	0.2027	0.2511	0.9731	0.8142	-0.6071	-0.4882
$[Nn_z\Delta]=[503]$										
β	0.1	0.2	0.3	0.4						
Energy [MeV]	-0.3942	0.3358	1.3713	2.5881						
ν	j	l								
1	11/2	5	0.0138	-0.0322	-0.1024	-0.1571				
1	9/2	5	0.9765	0.8268	0.6318	0.5260				
2	7/2	3	0.2153	0.5615	0.7683	0.8358				
$N=5 \quad \Omega=9/2$										
$[Nn_z\Delta]=[514]$				$[Nn_z\Delta]=[505]$						
β	0.1	0.2	0.3	0.4	0.1	0.2	0.3	0.4		
Energy [MeV]	-6.5708	-5.7286	-4.7404	-3.6068	0.2461	1.5424	3.0586	4.7954		
ν	j	l								
1	11/2	5	0.9995	0.9981	0.9958	0.9929	0.0314	0.0620	0.0912	0.1186
1	9/2	5	-0.0314	-0.0620	-0.0912	-0.1186	0.9995	0.9981	0.9958	0.9929
$N=5 \quad \Omega=11/2$										
$[Nn_z\Delta]=[505]$										
β	0.1	0.2	0.3	0.4						
Energy [MeV]	-5.7837	-4.0688	-2.1212	0.0592						
ν	j	l								
1	11/2	5	1.0000	1.0000	1.0000	1.0000				
Neutron mixing coefficients										
$N=5 \quad \Omega=1/2$										
$[Nn_z\Delta]=[550]$				$[Nn_z\Delta]=[541]$						
β	0.1	0.2	0.3	0.4	0.1	0.2	0.3	0.4		
Energy [MeV]	-15.8551	-16.8342	-17.8178	-18.8683	-10.6582	-11.9751	-13.3419	-14.4687		
ν	j	l								
1	11/2	5	0.9777	0.9167	0.8194	0.6911	-0.1994	-0.3208	-0.4087	-0.4847
1	9/2	5	-0.0079	-0.0170	-0.0300	-0.0466	-0.1476	-0.3087	-0.3287	-0.3125
2	7/2	3	0.2077	0.3836	0.5233	0.6145	0.8746	0.5736	0.3136	0.0938
2	5/2	3	-0.0040	-0.0196	-0.0532	-0.1046	-0.1196	-0.3439	-0.4632	-0.5182
3	3/2	1	0.0293	0.1064	0.2174	0.3414	0.3865	0.5299	0.5221	0.4583
3	1/2	1	-0.0030	-0.0207	-0.0611	-0.1227	-0.0991	-0.2717	-0.3734	-0.4242

TABLE VII (continued)

$N=5 \quad \Omega=1/2$ (continued)									
		$[Nn_z\Lambda]=[530]$				$[Nn_z\Lambda]=[521]$			
β		0.1	0.2	0.3	0.4	0.1	0.2	0.3	0.4
Energy [MeV]		-9.9910	-10.8857	-11.4536	-11.6609	-8.0306	-8.4822	-8.4270	-8.0017
ν	$j \quad l$								
1	11/2 5	-0.0320	-0.1730	-0.3072	-0.4146	0.0523	0.1416	0.2188	0.2813
1	9/2 5	0.9182	0.7369	0.6209	0.5495	0.2438	0.4726	0.5678	0.6124
2	7/2 3	0.1884	0.4136	0.4240	0.3566	-0.3422	-0.4655	-0.4898	-0.4802
2	5/2 3	0.3357	0.4426	0.4536	0.4561	-0.4143	-0.3469	-0.2514	-0.1736
3	3/2 1	0.0324	0.2197	0.3574	0.4331	0.6413	0.3657	0.2238	0.1400
3	1/2 1	0.0809	0.1084	0.0829	0.0585	-0.4875	-0.5345	-0.5259	-0.5154
		$[Nn_z\Lambda]=[510]$				$[Nn_z\Lambda]=[501]$			
β		0.1	0.2	0.3	0.4	0.1	0.2	0.3	0.4
Energy [MeV]		-6.9300	-6.5178	-5.7519	-4.7316	-5.0955	-3.8213	-2.3886	-0.8224
ν	$j \quad l$								
1	11/2 5	0.0229	0.0786	0.1330	0.1825	0.0075	0.0232	0.0400	0.0564
1	9/2 5	-0.2554	-0.3370	-0.3826	-0.4175	0.1015	0.1564	0.1919	0.2211
2	7/2 3	-0.1871	-0.3488	-0.4282	-0.4712	-0.0652	-0.1199	-0.1573	-0.1840
2	5/2 3	0.6952	0.5696	0.5154	0.4789	-0.4669	-0.4905	-0.4981	-0.5030
3	3/2 1	0.6080	0.6509	0.6193	0.5827	0.2602	0.3197	0.3446	0.3559
3	1/2 1	0.2151	0.1023	0.0583	0.0395	0.8365	0.7860	0.7550	0.7310
$N=5 \quad \Omega=3/2$									
		$[Nn_z\Lambda]=[541]$				$[Nn_z\Lambda]=[532]$			
β		0.1	0.2	0.3	0.4	0.1	0.2	0.3	0.4
Energy [MeV]		-15.6761	-16.4258	-17.0640	-17.5638	-10.2131	-10.8392	-11.3553	-11.6542
ν	$j \quad l$								
1	11/2 5	0.9821	0.9388	0.8816	0.8168	-0.1785	-0.2708	0.3298	0.3765
1	9/2 5	-0.0223	-0.0429	-0.0603	-0.0736	-0.3546	-0.5805	0.6185	0.6119
2	7/2 3	0.1862	0.3359	0.4535	0.5453	0.8694	0.6032	-0.4330	-0.3135
2	5/2 3	-0.0079	-0.0284	-0.0560	-0.0864	-0.1865	-0.3814	0.4842	0.5461
3	3/2 1	0.0175	0.0558	0.1019	0.1500	0.2276	0.2834	-0.2946	-0.2957
		$[Nn_z\Lambda]=[521]$				$[Nn_z\Lambda]=[512]$			
β		0.1	0.2	0.3	0.4	0.1	0.2	0.3	0.4
Energy [MeV]		-9.6332	-9.8426	-9.6900	-9.2217	-6.7747	-6.2403	-5.4370	-4.3961
ν	$j \quad l$								
1	11/2 5	-0.0515	-0.1949	-0.3089	-0.3971	0.0315	-0.0797	-0.1249	-0.1653
1	9/2 5	0.8969	0.7072	0.6192	0.5785	0.1929	-0.3433	-0.4234	-0.4751
2	7/2 3	0.3812	0.6164	0.6374	0.6031	-0.2367	0.3251	0.3700	0.3955
2	5/2 3	0.2065	0.1935	0.1684	0.1584	-0.6337	0.7062	0.6906	0.6625
3	3/2 1	0.0700	0.2108	0.2914	0.3448	0.7101	-0.5210	-0.4374	-0.3894
		$[Nn_z\Lambda]=[501]$							
β		0.1	0.2	0.3	0.4				
Energy [MeV]		-5.9177	-4.7184	-3.3251	-1.7943				
ν	$j \quad l$								
1	11/2 5	0.0071	0.0309	0.0550	0.0779				
1	9/2 5	-0.1791	-0.2077	-0.2263	-0.2446				
2	7/2 3	-0.0902	-0.1938	-0.2522	-0.2902				
2	5/2 3	0.7218	0.5636	0.5070	0.4800				
3	3/2 1	0.6624	0.7750	0.7906	0.7871				
$N=5 \quad \Omega=7/2$									
		$[Nn_z\Lambda]=[523]$				$[Nn_z\Lambda]=[514]$			
β		0.1	0.2	0.3	0.4	0.1	0.2	0.3	0.4
Energy [MeV]		-14.8023	-14.6105	-14.2759	-13.7856	-8.7499	-8.0876	-7.2736	-6.2869
ν	$j \quad l$								
1	11/2 5	0.9949	0.9839	0.9707	0.9566	0.0866	0.1274	0.1643	0.1955
1	9/2 5	-0.0407	-0.0771	-0.1084	-0.1350	0.8154	0.9351	0.9507	0.9545
2	7/2 3	0.0926	0.1610	0.2144	0.2583	-0.5724	-0.3307	-0.2629	-0.2252
		$[Nn_z\Lambda]=[503]$							
β		0.1	0.2	0.3	0.4				
Energy [MeV]		-8.3175	-6.9076	-5.2946	-3.5125				
ν	$j \quad l$								
1	11/2 5	-0.0522	-0.1250	-0.1754	-0.2162				
1	9/2 5	0.5775	0.3459	0.2904	0.2659				
2	7/2 3	0.8147	0.9299	0.9407	0.9394				

TABLE VII (continued)

$N=5 \quad \Omega=9/2$									
		$[Nn_z\Delta]=[514]$				$[Nn_z\Delta]=[505]$			
β		0.1	0.2	0.3	0.4	0.1	0.2	0.3	0.4
Energy [MeV]		-14.1081	-13.1755	-12.0783	-10.8161	-7.8043	-6.2684	-4.4725	-2.4171
ν	$j \quad l$								
1	11/2 5	0.9992	0.9972	0.9942	0.9906	0.0389	0.0749	0.1077	0.1368
1	9/2 5	-0.0389	-0.0749	-0.1077	-0.1368	0.9992	0.9972	0.9942	0.9906
$N=5 \quad \Omega=11/2$									
		$[Nn_z\Delta]=[505]$							
β		0.1	0.2	0.3	0.4				
Energy [MeV]		-13.2345	-11.3241	-9.1446	-6.6961				
ν	$j \quad l$								
1	11/2 5	1.0000	1.0000	1.0000	1.0000				
$N=6 \quad \Omega=1/2$									
		$[Nn_z\Delta]=[660]$				$[Nn_z\Delta]=[651]$			
β		0.1	0.2	0.3	0.4	0.1	0.2	0.3	0.4
Energy [MeV]		-9.2461	-10.4452	-11.7966	-13.4052	-3.6893	-4.8089	-5.7768	-6.4344
ν	$j \quad l$								
1	13/2 6	0.9792	0.9193	0.8236	0.7084	-0.1949	-0.3593	-0.5008	-0.6019
1	11/2 6	-0.0046	-0.0082	-0.0104	-0.0115	-0.0092	-0.0104	-0.0089	-0.0072
2	9/2 4	0.2008	0.3780	0.5210	0.6150	0.8913	0.6969	0.4893	0.2816
3	5/2 2	0.0291	0.1075	0.2181	0.3330	0.4001	0.5883	0.6563	0.6624
4	1/2 0	0.0027	0.0183	0.0509	0.0942	0.0862	0.1977	0.2811	0.3459
		$[Nn_z\Delta]=[640]$				$[Nn_z\Delta]=[631]$			
β		0.1	0.2	0.3	0.4	0.1	0.2	0.3	0.4
Energy [MeV]		-1.3469	-1.5413	-1.4655	-1.1598	-0.9858	-1.2711	-1.1366	-0.5840
ν	$j \quad l$								
1	13/2 6	0.0540	0.1514	0.2477	0.3373	0.0015	-0.0079	-0.0215	-0.0253
1	11/2 6	0.0222	0.0776	0.1046	0.0876	0.9997	0.9969	0.9944	0.9961
2	9/2 4	-0.3803	-0.5493	-0.6039	-0.6031	0.0172	0.0523	0.0721	0.0605
3	5/2 2	0.7616	0.5371	0.3582	0.2047	-0.0119	-0.0329	-0.0274	-0.0068
4	1/2 0	0.5215	0.6171	0.6593	0.6877	-0.0128	-0.0482	-0.0687	-0.0593
		$[Nn_z\Delta]=[620]$							
β		0.1	0.2	0.3	0.4				
Energy [MeV]		-0.0407	-0.5283	-1.1754	-1.9012				
ν	$j \quad l$								
1	13/2 6	-0.0165	-0.0522	-0.0953	-0.1464				
1	11/2 6	0.0024	0.0031	0.0034	0.0039				
2	9/2 4	0.1427	0.2590	0.3454	0.4184				
3	5/2 2	-0.5088	-0.5939	-0.6266	-0.6391				
4	1/2 0	0.8488	0.7599	0.6921	0.6285				
$N=6 \quad \Omega=3/2$									
		$[Nn_z\Delta]=[651]$				$[Nn_z\Delta]=[642]$			
β		0.1	0.2	0.3	0.4	0.1	0.2	0.3	0.4
Energy [MeV]		-9.0950	-10.0880	-11.0975	-12.1466	-3.3635	-3.9231	-4.2198	-4.1909
ν	$j \quad l$								
1	13/2 6	0.9821	0.9350	0.8675	0.7900	-0.1842	-0.3395	-0.4690	-0.5689
1	11/2 6	-0.0134	-0.0241	-0.0313	-0.0353	-0.0298	-0.0423	-0.0471	-0.0511
2	9/2 4	0.1866	0.3456	0.4747	0.5723	0.9294	0.8117	0.6837	0.5516
3	5/2 2	0.0221	0.0758	0.1450	0.2171	0.3183	0.4734	0.5571	0.6079
		$[Nn_z\Delta]=[631]$				$[Nn_z\Delta]=[622]$			
β		0.1	0.2	0.3	0.4	0.1	0.2	0.3	0.4
Energy [MeV]		-0.8516	-1.0482	-0.8740	-0.3291	-0.6690	-0.1887	0.4827	1.3058
ν	$j \quad l$								
1	13/2 6	0.0114	0.0131	0.0124	0.0096	0.0379	0.1017	0.1652	0.2284
1	11/2 6	0.9947	0.9977	0.9974	0.9969	-0.0976	-0.0481	-0.0443	-0.0473
2	9/2 4	-0.0009	0.0201	0.0226	0.0197	-0.3183	-0.4705	-0.5537	-0.6065
3	5/2 2	0.1022	0.0641	0.0671	0.0749	0.9422	0.8752	0.8149	0.7601

TABLE VII (continued)

$N=6 \quad \Omega=5/2$										
		$[Nn_z\Delta]=[642]$				$[Nn_z\Delta]=[633]$				
β	0.1	0.2	0.3	0.4	0.1	0.2	0.3	0.4		
Energy [MeV]	-8.7969	-9.4294	-9.9717	-10.4113	-2.8363	-2.7568	-2.4321	-1.8587		
ν	j	l								
1	13/2	6	0.9868	0.9554	0.9144	0.8685	-0.1601	-0.2905	-0.3959	-0.4803
1	11/2	6	-0.0213	-0.0390	-0.0519	-0.0604	-0.0531	-0.0934	-0.1269	-0.1585
2	9/2	4	0.1600	0.2902	0.3957	0.4816	0.9660	0.9057	0.8365	0.7615
3	5/2	2	0.0119	0.0376	0.0684	0.1007	0.1962	0.2942	0.3570	0.4054
$[Nn_z\Delta]=[622]$										
β	0.1	0.2	0.3	0.4	0.1	0.2	0.3	0.4		
Energy [MeV]	-0.5702	-0.5582	-0.2500	0.3530	-0.0275	0.8667	1.8112	2.7915		
ν	j	l								
1	13/2	6	0.0131	0.0114	-0.0009	-0.0214	0.0195	0.0513	0.0848	0.1208
1	11/2	6	0.9979	0.9946	0.9903	0.9853	-0.0295	-0.0246	-0.0227	-0.0217
2	9/2	4	0.0490	0.0891	0.1197	0.1430	-0.1973	-0.2958	-0.3597	-0.4096
3	5/2	2	0.0397	0.0527	0.0707	0.0913	0.9797	0.9536	0.9289	0.9040
$N=6 \quad \Omega=7/2$										
		$[Nn_z\Delta]=[633]$				$[Nn_z\Delta]=[624]$				
β	0.1	0.2	0.3	0.4	0.1	0.2	0.3	0.4		
Energy [MeV]	-8.3556	-8.5011	-8.5094	-8.3625	-2.1752	-1.4471	-0.5518	0.4902		
ν	j	l								
1	13/2	6	0.9920	0.9744	0.9524	0.9284	-0.1246	-0.2244	-0.3046	-0.3665
1	11/2	6	-0.0274	-0.0515	-0.0712	-0.0866	-0.0743	-0.1575	-0.2572	-0.3736
2	9/2	4	0.1228	0.2189	0.2963	0.3614	0.9894	0.9617	0.9171	0.8521
$[Nn_z\Delta]=[613]$										
β	0.1	0.2	0.3	0.4						
Energy [MeV]	-0.1316	0.2561	0.8819	1.7486						
ν	j	l								
1	13/2	6	0.0180	0.0150	-0.0109	-0.0613				
1	11/2	6	0.9969	0.9862	0.9637	0.9235				
2	9/2	4	0.0771	0.1651	0.2667	0.3786				
$N=6 \quad \Omega=9/2$										
		$[Nn_z\Delta]=[624]$				$[Nn_z\Delta]=[615]$				
β	0.1	0.2	0.3	0.4	0.1	0.2	0.3	0.4		
Energy [MeV]	-7.7720	-7.2997	-6.6761	-5.8931	-1.4205	-0.0494	1.3939	2.9088		
ν	j	l								
1	13/2	6	0.9966	0.9892	0.9797	0.9689	-0.0783	-0.1430	-0.1992	-0.2473
1	11/2	6	-0.0304	-0.0588	-0.0844	-0.1073	-0.0795	-0.1826	-0.3060	-0.4252
2	9/2	4	0.0761	0.1344	0.1819	0.2228	0.9937	0.9727	0.9310	0.8706
$[Nn_z\Delta]=[604]$										
β	0.1	0.2	0.3	0.4						
Energy [MeV]	0.4827	1.4632	2.6641	4.0777						
ν	j	l								
1	13/2	6	0.0242	0.0326	0.0229	-0.0013				
1	11/2	6	0.9964	0.9814	0.9483	0.8987				
2	9/2	4	0.0816	0.1891	0.3166	0.4386				
$N=6 \quad \Omega=11/2$										
		$[Nn_z\Delta]=[615]$				$[Nn_z\Delta]=[606]$				
β	0.1	0.2	0.3	0.4	0.1	0.2	0.3	0.4		
Energy [MeV]	-7.0427	-5.7931	-4.3611	-2.7470	1.2952	3.1412	5.2592	7.6493		
ν	j	l								
1	13/2	6	0.9996	0.9985	0.9969	0.9947	0.0276	0.0541	0.0792	0.1025
1	11/2	6	-0.0276	-0.0541	-0.0792	-0.1025	0.9996	0.9985	0.9969	0.9947
$N=6 \quad \Omega=13/2$										
		$[Nn_z\Delta]=[606]$								
β	0.1	0.2	0.3	0.4						
Energy [MeV]	-6.1612	-3.9364	-1.4347	1.3439						
ν	j	l								
1	13/2	6	1.0000	1.0000	1.0000	1.0000				

APPENDIX

Nilsson³ has given the expressions for the electromagnetic transition in the $(i\Lambda\Sigma)$ representation. In the case of an r -dependent spin-orbit potential considered here one has to choose the $(j\lambda K)$ representation for the spherical basis.

The electric and the magnetic multipole operators in the laboratory system are given by

$$\mathbf{M}(E\lambda, \mu) = \sum_p \left(e_{\text{eff}} + (-)^{\lambda} \frac{Z}{A^{\lambda}} e \right) r_p^{\lambda} Y_{\lambda\mu}(\theta_p, \Phi_p) + (3/4\pi) Z e R_0^{\lambda} \alpha_{\lambda\mu}^{\dagger}, \quad (36)$$

$$\mathbf{M}(M\lambda, \mu) = \frac{e\hbar}{2mc} \sum_p \left(g_s s_{\mu} + \frac{2}{\lambda+1} g_l l_{\mu} \right)_p \nabla_p [r_p^{\lambda} Y_{\lambda\mu}(\theta_p, \phi_p)] + \frac{e\hbar}{mc} \frac{1}{\lambda+1} g_R \int \mathbf{R}(\mathbf{r}) \nabla [r^{\lambda} Y_{\lambda\mu}(\theta, \phi)] d\tau. \quad (37)$$

The first term gives the single-particle operator, which sums over the transforming nucleons p . The effective charge e_{eff} depends on the multipolarity and on the charge of the nucleon. The multipole deformation parameters $\alpha_{\lambda\mu}$ are defined in Eq. (16). The symbol R_0 is the nuclear radius and $R(r)$ is the collective angular momentum density.

For magnetic dipole transitions the operator has an especially simple form

$$\begin{aligned} \mathbf{M}(M1, \mu) &= \frac{e\hbar}{2mc} [g_R I_{\mu} + (g_l - g_R) l_{\mu} + (g_s - g_R) s_{\mu}] \\ &= \frac{e\hbar}{2mc} [g_R I_{\mu} + (g_l - g_s) l_{\mu} + (g_s - g_R) j_{\mu}]. \end{aligned} \quad (38)$$

The letters g_R , g_s , g_l indicate the collective, the spin, and the orbital angular momentum g factors

$$\begin{aligned} g_s &= \begin{cases} 5.59 & \text{for a proton} \\ -3.83 & \text{for a neutron,} \end{cases} \\ g_l &= \begin{cases} 1 & \text{for a proton} \\ 0 & \text{for a neutron,} \end{cases} \\ g_R &= \frac{Z}{A}. \end{aligned} \quad (39)$$

The value for g_R is only correct in the hydrodynamic approximation. The experiment yields smaller values.^{24, 33-35} In the expression for the transition probability

$$T(\lambda) = \frac{8\pi(\lambda+1)}{\lambda[(2\lambda+1)!!]^2} \frac{1}{\hbar} \left(\frac{E_{if}}{\hbar c} \right)^{2\lambda+1} B(\lambda), \quad (40)$$

the reduced probability is defined by

$$B(\lambda; I_i N_i K_i \rightarrow I_f N_f K_f) = (1/\hat{I}_i) |\langle I_f N_f K_f | \mathbf{m}(\lambda) | I_i N_i K_i \rangle|^2. \quad (41)$$

We have used the reduced matrix element as in the definition of Edmonds.¹⁰ A very useful connection between the transition probability for $\lambda=1$ and for $\lambda=2$ and the reduced probability is

$$\begin{aligned} T(1)[1/\text{sec}] &= 1.59 \times 10^8 (E_{if}[\text{keV}])^3 B(1)[10^{-24} \text{cm}^2 e^2], \\ T(2)[1/\text{sec}] &= 1.23 \times 10^{-2} (E_{if}[\text{keV}])^5 \times B(2)[10^{-48} \text{cm}^4 e^2]. \end{aligned} \quad (42)$$

To calculate the reduced matrix elements one has to transform the multipole operators into the intrinsic system.

$$\mathbf{M}(\lambda, \mu) = \sum_{\rho} D_{\mu\rho}^{\lambda} \mathbf{M}(\lambda, \rho) \quad (43)$$

³³ E. Bodendstedt, Fortschr. Physik **10**, 321 (1962).

³⁴ A. Faessler and W. Greiner, Z. Physik **177**, 190 (1964).

³⁵ W. Greiner, Phys. Rev. Letters **14**, 599 (1965).

$$\begin{aligned}
\langle I_f N_f K_f || \mathbf{M}(E\lambda) || I_i N_i K_i \rangle = & \left(e_{\text{eff}} + (-)^{\lambda} \frac{Z}{A^{\lambda}} e \right) (\hat{I}_i / \hat{I}_f)^{1/2} (-)^{\lambda - I_i - \frac{1}{2}} \\
& \times \sum_{j_i j_f} c_{j_i} c_{j_f} (\hat{l}_i \hat{l}_f \hat{j}_i \hat{j}_f / (4\pi))^{1/2} \begin{pmatrix} l_i & \lambda & l_f \\ 0 & 0 & 0 \end{pmatrix} \begin{Bmatrix} j_i & \lambda & j_f \\ l_f & \frac{1}{2} & l_i \end{Bmatrix} \left[\begin{pmatrix} I_i & \lambda & I_f \\ K_i & -K_i + K_f & -K_f \end{pmatrix} \begin{pmatrix} j_i & \lambda & j_f \\ K_i & -K_i + K_f & -K_f \end{pmatrix} \right. \\
& \left. + (-)^{I_f - \frac{1}{2}} \Pi_f \begin{pmatrix} I_i & \lambda & I_f \\ K_i & -K_i - K_f & K_f \end{pmatrix} \begin{pmatrix} j_i & \lambda & j_f \\ K_i & -K_i - K_f & K_f \end{pmatrix} \right] \langle N_f j_f l_f | r^{\lambda} | N_i j_i l_i \rangle (\hbar/m\omega)^{\lambda/2}. \quad (44)
\end{aligned}$$

Here the abbreviation $\hat{l} \equiv 2l+1$ is used and it is assumed that the radial matrix elements

$$\langle N_f j_f l_f | r^{\lambda} | N_i j_i l_i \rangle \quad (45)$$

are calculated in oscillator units $(\hbar/m\omega_0)^{\lambda/2}$. The r^2 matrix elements are tabulated (in Table V) for the Saxon-Woods and oscillator functions of the rare-earth region. For other powers of r the matrix elements can be calculated using the expansion of the Saxon-Woods functions in Table II. For the oscillator functions a general formula is given in Eq. (10). For the calculation of the reduced $M1$ matrix element,

$$\begin{aligned}
\langle I_f N_f K_f || \mathbf{M}(M1) || I_i N_i K_i \rangle = & g_R [\hat{I}(I+1)I]^{1/2} \delta_{I_i; I_f} \delta_{N_i; N_f} \delta_{K_i; K_f} \delta_{\alpha_i; \alpha_f} + [\hat{I}_i / \hat{I}_f]^{1/2} \sum_{j_i j_f} c_{j_i} c_{j_f} \\
& \times (-)^{I_i - I_i - K_f} \left[\begin{pmatrix} I_i & 1 & I_f \\ K_i & K_f - K_i & -K_f \end{pmatrix} \begin{pmatrix} j_i & 1 & j_f \\ K_i & K_f - K_i & -K_f \end{pmatrix} + \delta_{K_i K_f; 1/2} (-)^{I_f - \frac{1}{2}} \Pi_f \right. \\
& \times \left. \begin{pmatrix} I_i & 1 & I_f \\ \frac{1}{2} & -1 & \frac{1}{2} \end{pmatrix} \begin{pmatrix} j_i & 1 & j_f \\ \frac{1}{2} & -1 & \frac{1}{2} \end{pmatrix} \right] \left[(g_s - g_R) (-)^{j_i - K_f} [\hat{j}_i(j_i+1)j_i]^{1/2} \delta_{j_i; j_f} \delta_{K_i; K_f} \right. \\
& \left. + (g_s - g_l) [\hat{l}_i(l_i+1)l_i]^{1/2} (-)^{\frac{1}{2} + l_f - K_f} [\hat{j}_i \hat{j}_f]^{1/2} \begin{Bmatrix} j_i & 1 & j_f \\ l_i & \frac{1}{2} & l_i \end{Bmatrix} \delta_{l_i; l_f} \right] \left(\frac{e\hbar}{2mc} \right), \quad (46)
\end{aligned}$$

the last expression of Eq. (38) was used. The Greek subscript α labels the different wave functions for the same N and K . The symbol $\delta_{\alpha_i; \alpha_f}$ indicates that this term applies only to the same initial and final intrinsic states. The reduced $M1$ transition probability between the state I and $I-1$ in the same rotational band is given by the expression

$$B(M1; INK \rightarrow I-1, N, K) = \left(\frac{e\hbar}{2mc} \right)^2 (g_K - g_R)^2 K^2 \frac{(I-K)(I+K)}{I(2I+1)}. \quad (47)$$

The g_K factor defined by the equation

$$\langle NK\alpha | (g_s - g_R) s_0 + (g_l - g_R) l_0 | NK\alpha \rangle = K(g_K - g_R) \quad (48)$$

is

$$g_K = g_s + K^{-1}(g_l - g_s) \sum_{j_i j_f} \delta_{l_i l_f} c_{j_i} c_{j_f} (\hat{j}_i \hat{j}_f)^{1/2} (-)^{\frac{1}{2} + l - K} \begin{Bmatrix} j_i & 1 & j_f \\ l & \frac{1}{2} & l \end{Bmatrix} \begin{pmatrix} j_i & 1 & j_f \\ K & 0 & K \end{pmatrix} (l(l+1)l)^{1/2}. \quad (49)$$